Dating basal peat: The geochronology of peat initiation revisited

Quik, C., Palstra, S. W. L., van Beek, R., van der Velde, Y., Candel, J. H. J., van der Linden, M., Kubiak-Martens, L., Swindles, G. T., Makaske, B., & Wallinga, J. (2022). Dating basal peat: The geochronology of peat initiation revisited. *Quaternary Geochronology*, Article 101278. Advance online publication. https://doi.org/10.1016/j.quageo.2022.101278

Published in:
Quaternary Geochronology

Document Version:
Peer reviewed version

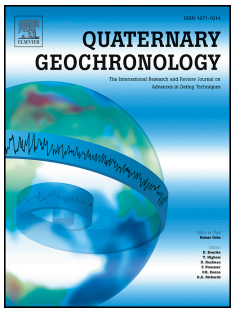

Dating basal peat: The geochronology of peat initiation revisited

Cindy Quik, Sanne W.L. Palstra, Roy van Beek, Ype van der Velde, Jasper H.J. Candel, Marjolein van der Linden, Lucy Kubiak-Martens, Graeme T. Swindles, Bart Makaske, Jakob Wallinga

PII: S1871-1014(22)00026-7

DOI: https://doi.org/10.1016/j.quageo.2022.101278

Reference: QUAGEO 101278

To appear in: *Quaternary Geochronology*

Received Date: 24 November 2021

Revised Date: 15 March 2022

Accepted Date: 21 March 2022

Please cite this article as: Quik, C., Palstra, S.W.L., van Beek, R., van der Velde, Y., Candel, J.H.J., van der Linden, M., Kubiak-Martens, L., Swindles, G.T., Makaske, B., Wallinga, J., Dating basal peat: The geochronology of peat initiation revisited, *Quaternary Geochronology* (2022), doi: https://doi.org/10.1016/j.quageo.2022.101278.

Dating basal peat: the geochronology of peat initiation revisited

Cindy Quik[1]*, Sanne W.L. Palstra[2], Roy van Beek[1,3], Ype van der Velde[4], Jasper H.J. Candel[1], Marjolein van der Linden[5], Lucy Kubiak-Martens[5], Graeme T. Swindles[6,7], Bart Makaske[1], Jakob Wallinga[1]

[1] *Soil Geography and Landscape Group, Wageningen University & Research, Wageningen, the Netherlands*
[2] *Centre for Isotope Research, Energy and Sustainability Research Institute Groningen, University of Groningen, Groningen, the Netherlands*
[3] *Cultural Geography Group, Wageningen University & Research, Wageningen, the Netherlands*
[4] *Faculty of Science, Earth and Climate, Vrije Universiteit Amsterdam, Amsterdam, the Netherlands*
[5] *BIAX Consult, Zaandam, the Netherlands*
[6] *Geography, School of Natural and Built Environment, Queen's University Belfast, Belfast, United Kingdom*
[7] *Ottawa-Carleton Geoscience Centre and Department of Earth Sciences, Carleton University, Ottawa, Ontario, Canada*

CQ	https://orcid.org/0000-0002-7112-0195	MvdL	https://orcid.org/0000-0001-9281-0892
SP	https://orcid.org/0000-0003-2024-0872	LKM	https://orcid.org/0000-0002-5322-3211
YvdV	https://orcid.org/0000-0002-2183-2573	GS	https://orcid.org/0000-0001-8039-1790
JC	https://orcid.org/0000-0001-8365-8673	RvB	https://orcid.org/0000-0002-0726-6974
BM	https://orcid.org/0000-0002-2777-3017	JW	https://orcid.org/0000-0003-4061-3066

* Corresponding author:
cindy.quik@wur.nl
Wageningen University & Research
Soil Geography and Landscape Group
Postbus 47, 6700 AA, Wageningen

Abstract Attributing the start of peat growth to an absolute timescale requires dating the bottom of peat deposits overlying mineral sediment, often called the *basal peat*. Peat initiation is reflected in the stratigraphy as a gradual transition from mineral sediment to increasingly organic material, up to where it is called peat. So far, varying criteria have been used to define basal peat, resulting in divergent approaches to date peat initiation. The lack of a universally applicable and quantitative definition, combined with multiple concerns that have been raised previously regarding the radiocarbon dating of peat, may result in apparent ages that are either too old or too young for the timing of peat initiation. Here, we aim to formulate updated recommendations for dating peat initiation. We provide a conceptual framework that supports the use of the organic matter (OM) gradient for a quantitative and reproducible definition of the mineral-to-peat transition (i.e., the stratigraphical range reflecting the timespan of the peat initiation process) and the layer defined as *basal peat* (i.e., the stratigraphical layer that is defined as the bottom of a peat deposit). Selection of dating samples is often challenging due to poor preservation of plant macrofossils in basal peat, and the representativity of humic and humin dates for the age of basal peat is uncertain. We therefore analyse the mineral-to-peat transition based on three highly detailed sequences of radiocarbon dates, including dates of plant macrofossils and the humic and humin fractions obtained from bulk samples. Our case study peatland in the Netherlands currently harbours a bog vegetation, but biostratigraphical analyses show that during peat initiation the vegetation was mesotrophic. Results show that plant macrofossils provide the most accurate age in the mineral-to-peat transition and are therefore recommendable to use for ^{14}C dating basal peat. If these are unattainable, the humic fraction provides the best alternative and is interpreted as a terminus-ante-quem for peat initiation. The potential large age difference between dates of plant macrofossils and humic or humin dates (up to ~1700 years between macrofossil and humic ages, and with even larger differences for humins) suggests that studies reusing existing bulk dates of basal peat should take great care in data interpretation. The potentially long timespan of the peat initiation process (with medians of ~1000, ~1300 and ~1500 years within our case study peatland) demonstrates that choices regarding sampling size and resolution need to be well substantiated. We summarise our findings as a set of recommendations for dating basal peats, and advocate the widespread use of OM determination to obtain a low-cost, quantitative and reproducible definition of *basal peat* that eases intercomparison of studies.

Key words (alphabetical) Accelerator Mass Spectrometry (AMS), bulk, humics, humins, organic matter, peat initiation, peat remnant, plant macrofossils, radiocarbon, stratigraphy.

1 Introduction

The start of peat growth represents a major landscape change. Attributing this transition to an absolute timescale requires dating the bottom of peat deposits overlying mineral sediment, often called the *basal peat*. Robust age control of basal peat layers is of paramount importance, not only for studies aimed directly at peatlands, for instance concerning their palaeogeography, development and carbon sequestration (e.g. Gorham *et al.*, 2007; Yu *et al.*, 2011), but also for interdisciplinary research fields that harness the peat archive for climate and sea level reconstructions (e.g. Törnqvist and Hijma, 2012; Morris *et al.*, 2018) or to contextualize wetland archaeology (e.g. Chapman *et al.*, 2013).

Peat growth results from a positive production-decay balance, i.e. where the decay rate of organic material is slower than the rate of production. The decay rate primarily depends on moisture level, which in turn is influenced by various factors such as climate (e.g. Weckström et al., 2010), changes in hydrological base level (sea level rise, e.g. Berendsen et al., 2007) or regional groundwater changes (e.g. van Asselen et al., 2017), landforms and surface topography (e.g. Almquist-Jacobson and Foster, 1995; Mäkilä, 1997; Loisel et al., 2013), impermeable deposits or resistant layers in the soil profile (e.g. Breuning-Madsen et al., 2018; Van der Meij et al., 2018), and anthropogenic influence (e.g. Moore, 1975; Moore, 1993).

A wetland is an area where the substrate is water-saturated or inundated for a substantial period (Charman, 2002a; Joosten and Clarke, 2002). A minimum depth of 30 cm of peat is required to classify a wetland area as a peatland (Charman, 2002a; Joosten and Clarke, 2002; Rydin and Jeglum, 2013a). This implies that during build-up of the first organic deposits, the area is not yet a peatland according to definition, but rather a wetland where peat formation occurs. As a result of these definitions, one could make a distinction between peat initiation (i.e., build-up of the first organic deposits) and peatland initiation (i.e., referring to the moment when 30 cm of organic deposits has formed in a certain area). In the current paper, we focus on peat initiation (prior to the formation of a peat layer with a thickness of 30 cm or more).

Peat initiation may occur through (a combination of) three processes, briefly outlined below based on Charman (2002a) and Rydin and Jeglum (2013a). Terrestrialisation (also called infilling) refers to the process where peat develops in or at the edge of water bodies. Terrestrialisation is characterized by gyttja deposits at the base, which require a water depth of at least 0.5 m to form (Bos, 2010). Paludification refers to peat formation on previously unsaturated mineral substrate, and thus reflects moistening of the landscape. Primary mire formation involves peat growth on newly exposed waterlogged substrate (e.g. after land uplift from sea). Here, peat growth starts directly on the fresh parent material.

When a peat surface rises above the regional groundwater level, consequent strong dependence on rainwater leads to ombrotrophication, which may result in a fen-bog transition (Charman, 2002c; Rydin and Jeglum, 2013b; Loisel and Bunsen, 2020). Peatlands not only grow vertically, but also expand laterally, which results in a larger peat-covered area. Paludification of surrounding soils due to poor drainage at the edge of the peatland, and resulting peatland expansion, is known as an autogenic process (Charman, 2002c). However, allogenic factors such as climate and topography influence the rate and extent of lateral spread (e.g. Korhola, 1994; Ruppel *et al.*, 2013).

Peat initiation can be studied at various scales (fig. 1a). At the landscape scale, peat initiation refers to the onset of peat growth at a certain locus, that expands over time to cover a larger area. In this case, the term *peat initiation* refers to the location and time where the nucleus of the resultant peatland developed. In contrast, at the very local scale, *peat initiation* may be used to indicate the moment of accumulation of the first peat deposits at a specific location, where the location may reflect a development locus but could also be a site that became covered by peat through lateral expansion of a nearby locus. To distinguish lateral expansion from a development locus, one or multiple transects of basal peat dates are usually required (e.g. Mäkilä, 1997; Mäkilä and Moisanen, 2007; Chapman et al., 2013). The approach for dating peat initiation at both scales is similar, while the research aim determines which scale level is of interest.

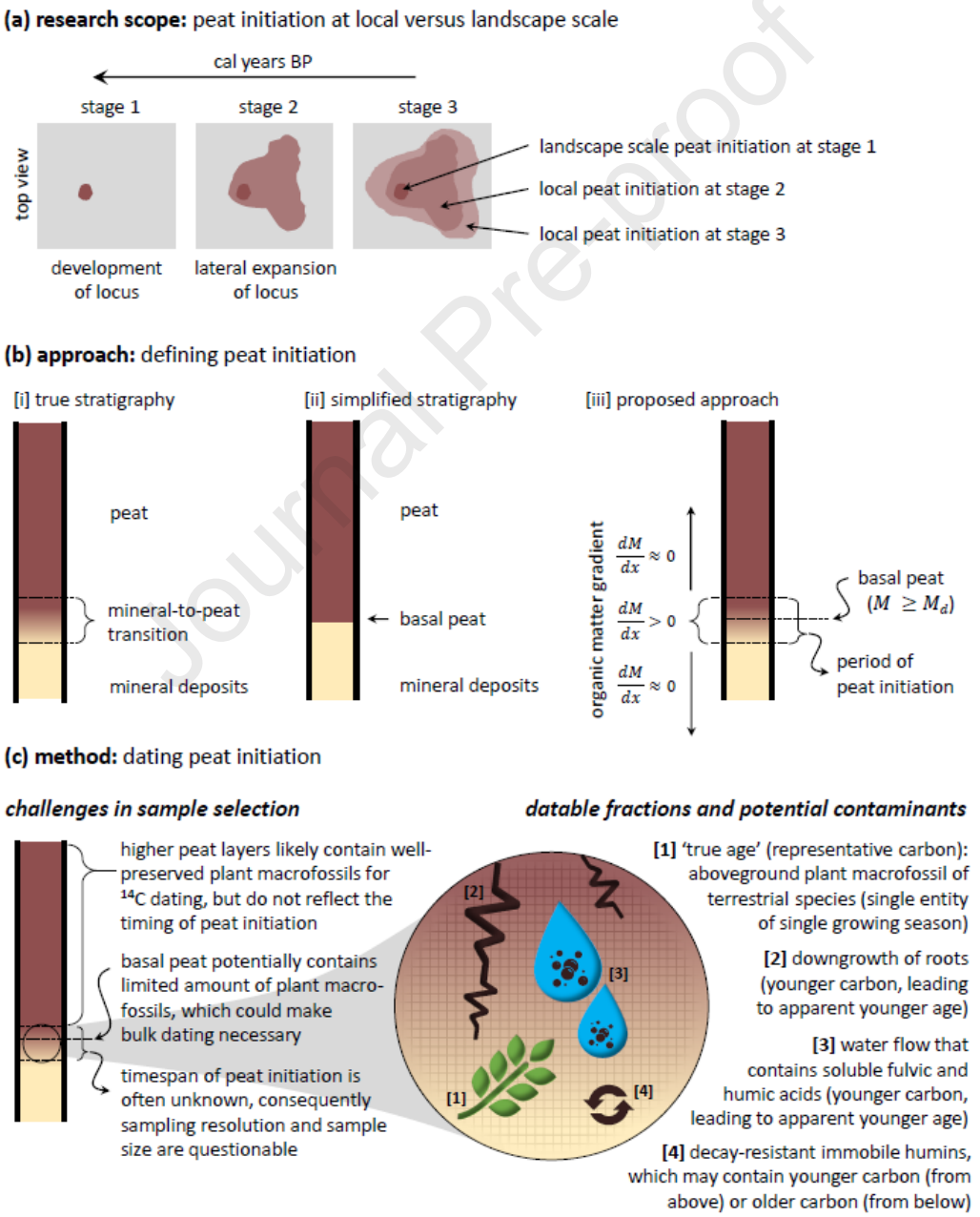

Figure 1. Conceptual framework for dating peat initiation. (a) Schematic top-view of a landscape (peat is indicated in brown), showing the meaning of *peat initiation* at both the landscape and local scales. (b) Schematic cores showing [i] stratigraphy

that results from peat initiation, [ii] simplified interpretation of this stratigraphy, and [iii] the approach we propose in this study. Here, we propose using the organic matter gradient to characterise the mineral-to-peat transition and to define *basal peat*. To qualify the material as peat, the OM content should be above a certain value denoted with M_d, where the first cm of material that has an OM content equal to or above M_d is defined as the *basal peat*. (c) Schematic core showing challenges with sample selection, and datable fractions and potential contaminants for ^{14}C dating *basal peat*.

[2-column fitting figure]

Peat initiation is a process that takes place during a certain timespan, which is reflected in the stratigraphy as a gradual transition from mineral sediment to increasingly organic material (fig. 1b), up to where it is called peat (depending on definitions used). We propose it would be most accurate to speak of a period of peat initiation, which requires a series of vertical dates that encloses the gradual stratigraphical boundary. However, a single date of *basal peat* is often used to reflect peat initiation, potentially for reasons of practicality or feasibility when there is need to date many sites. This requires however an unambiguous and explicit definition of *basal peat*.

So far, varying criteria have been used to define *basal peat*, resulting in divergent approaches to date the onset of peat accumulation (Quik *et al.*, 2021). Current approaches, which are partly dependent on the research objectives, vary from visual determinations and basic laboratory analyses such as loss-on-ignition (e.g. Edvardsson *et al.,* 2014) to detailed micromorphological analyses (e.g. Cubizolle *et al.*, 2007) and studies of plant macrofossils (e.g. Loisel *et al.*, 2013). Depending on the approach taken, the accuracy of resulting dates to represent peat initiation may be called into question, as the (possibly site-specific) definition of the *basal peat* often remains implicit.

The international soil classification of the World Reference Base for Soil Resources states that 'organic material' has ≥ 20% soil organic carbon in the fine earth fraction (by mass) (WRB-IUSS, 2015). A practical challenge of this definition is that determination of soil organic carbon requires expensive analyses (e.g. elemental analysis), whereas soil organic matter (which includes both organic carbon and, if present, inorganic carbon such as carbonates) can be measured with an inexpensive, simple protocol (loss-on-ignition).

To the best of our knowledge, both the mineral-to-peat transition and the layer called *basal peat* (the stratigraphical level used to reflect peat initiation), are not universally defined based on organic matter (OM) content. A universal definition eases inter-site comparisons, but a site-specific definition may be preferable to cover regional differences. Both require that the properties to define *basal peat* are explicit and reproducible. For example, Cubizolle *et al.* (2007) use 30% OM as lower limit for peat in the French Massif Central, whereas for instance Loisel *et al.* (2013) use 50% OM for an Alaskan peatland. To stimulate the use of quantitative and reproducible definitions, a property such as OM content is recommendable, as it can be measured relatively easily and at low cost. As there is a clear gradient in organic matter (indicated by the variable M) at the transition from mineral sediment to peat (i.e., as a function of distance x upwards in the profile), both the mineral-to-peat transition (i.e., the period of peat initiation) and the *basal peat* (i.e., the stratigraphical layer that is defined as the bottom of a peat deposit) can be defined by the organic matter content [$M(x)$] and the organic matter gradient [the derivative given by $\frac{dM}{dx}$] (fig. 1b).

After defining *basal peat*, adequate sampling and sample pre-treatment for radiocarbon dating are required to accurately derive the age of the basal peat layer. The discussion on which samples most accurately indicate the age of peat layers started several decades ago (e.g. Törnqvist *et al.*, 1992, 1998; Shore *et al.*, 1995; Nilsson *et al.*, 2001; Brock *et al.*, 2011; Van der Plicht *et al.*, 2019). Various studies have highlighted multiple concerns with the radiocarbon dating of peat. If carbon from other carbon sources is incorporated or mixed with the original sample material and cannot be removed (by manual selection and/or chemically), this may result in apparent ages that are either too old or too young for the peat layer of interest (table 1).

Table 1. Concerns with ^{14}C dating of peat samples. 'Organism' refers to a plant of peat-forming vegetation.

Processes when the organism was alive	***Processes after the organism died***
Apparent older age	*Apparent younger age*
Circumstances where organisms incorporate carbon from a reservoir that is not in equilibrium with the atmosphere (so-called reservoir effect), causing apparent ages that are too old: • This typically applies to aquatic samples from marine or freshwater circumstances (the latter is also known as hardwater effect, e.g. Törnqvist *et al.*, 1992; Philippsen, 2013). Relevance of a reservoir effect for peat samples has been postulated (Kilian *et al.*, 1995) but not confirmed (Blaauw *et al.*, 2004). Incorporation of older carbon or ^{14}C-depleted carbon may also occur through: • Decomposition of underlying peat layers and subsequent assimilation of CO_2 (Smolders *et al.*, 2001). • Assimilation of CH_4 originating from bacterial methanogenesis (Van der Plicht *et al.*, 2019).	Mixing with younger carbon through: • Downgrowth of roots (Törnqvist *et al.*, 1992). • Translocation of mobile humic acids downwards in a profile, followed by chemical break-down to humins (Palstra *et al.*, 2021). • Contamination during sample storage by microbial growth (Wohlfarth *et al.*, 1998) or laboratory pre-treatments. Small samples or samples with low carbon content are particularly sensitive to contamination (Van der Plicht *et al.*, 2019), especially if samples are older than 20 ka.

Bulk dating is often complicated by difficulties with interpreting the resulting age, which represents a mixture of ages of various organic fractions. The development of AMS in radiocarbon has enabled new possibilities for dating peat deposits due to much lower requirements regarding sample sizes (e.g. Tuniz *et al.*, 1998; Jull and Burr, 2015). The concerns outlined in table 1 have led to the recommendation to date short-lived, aboveground plant macrofossils of terrestrial species with AMS (e.g. Piotrowska *et al.*, 2011).

Unfortunately, AMS dating of terrestrial macrofossils is not always possible for mineral-to-peat transitions (fig. 1c). Depending on the type of mire and local circumstances, the basal peat layer may have an amorphous peat facies largely devoid of (identifiable) plant macrofossils. Limited presence of plant macrofossils may require resorting to bulk sampling for radiocarbon dating the basal peat layer, which could hamper interpretation of dating results. The magnitude of this problem appears to vary. For instance, Törnqvist et al. (1992) found age differences of up to 600 ^{14}C year between bulk and macrofossil samples from mid-latitude minerotrophic peats, whereas Berendsen et al. (2007), who studied comparable deposits, and Holmquist *et al.* (2016), who looked at basal peat from circum-arctic peatlands, reported no significant age differences. Depending on the duration of

the period in which the basal peat forms, sampling plant macrofossils from higher positions in the peat profile to circumvent bulk sampling at the base may no longer reflect peat initiation, as a potentially large age difference between these layers might exist.

Pre-treatment of bulk samples using acids and base solutions results in multiple organic fractions which are defined based on their solubilities (Brock *et al.*, 2011; Van der Plicht *et al.*, 2019): fulvic acids are soluble in both alkaline and acids, humic acids are soluble in alkaline but insoluble in acids, and humins are insoluble in alkaline and acids. Fulvic acids are usually removed during pre-treatment and not used for dating. Because of their high mobility, which allows them to translocate easily through a soil profile, significantly younger dates might be obtained for fulvics than for the humic and humin fraction from the same layer (Shore *et al.*, 1995). As the solubility of humics is determined by pH and lower under acidic conditions (Wüst *et al.*, 2008), their mobility depends on environmental circumstances and may change through time. There is no clear consensus in literature on whether humic or humin dates are most representative for dating peat layers. Examples range from studies where no significant age differences are reported (e.g. Cook *et al.*, 1998; Waller *et al.*, 2006), studies that consider humins to be most appropriate for peat (e.g. Hammond *et al.*, 1991; Van der Plicht *et al.*, 2019) and humics for deposits with low carbon amounts (Van der Plicht et al. 2019), or where a conclusion that one or the other fraction is more reliable could not be drawn unquestionably (Brock *et al.*, 2011). Moreover, hardly any studies focus on *basal peat* layers while investigating the ages of these organic fractions (with the exception of Brock *et al.*, 2011). It is therefore unknown which carbon fractions of these basal peat layers, which might be slightly different in organic carbon composition (especially in carbon content) compared to peat samples from higher positions in peat profiles, are most representative for the time period of peat initiation.

In the current study we aim to formulate recommendations for dating *basal peat*. Issues that we specifically address are (1) peat initiation is a process of a certain timespan rather than an event, (2) *basal peat* needs to be clearly defined, (3) selection of dating samples is typically challenging due to potential poor preservation of plant macrofossils in *basal peat* and (4) the representativity of humic and humin dates for the age of *basal peat* is questionable. We analyse lithological, biostratigraphical and geochronological characteristics of the mineral-to-peat transition in a bog remnant, focusing on understanding the course of the process of peat initiation and related implications for dating.

2 Methods

2.1 Selection of study area and overview of methods

The Fochteloërveen peat remnant (the Netherlands, fig. 2) was selected as case study region. This peatland, with its surface area of approximately 2,500 hectares, is one of the largest raised bog remnants of Northwest Europe. The area is considered representative for many (non-coastal) peatlands of the Northwest European Plain with regard to the widespread distribution of its mineral substrate and characteristic climatic conditions (see section 2.2). As many European peatlands are subject to ongoing excavation or affected by reclamation relics from historical peat-cutting, basal peat layers may be damaged. In the Fochteloërveen, several former peat cutting pits (some of which are currently artificial lakes) are present and superficial patterns of historical buckwheat fire culture can be recognized. However, the latter disturbed only the surface of the peatland and therefore basal peat layers are undamaged in the majority of the area. A recent study on peat initiation trends in the northern Dutch coversand landscape (Quik *et al.*, 2021) provides background information on peat growth in the wider study region, and demonstrated that the Fochteloërveen (as one of the few surviving bog remnants) has so far received limited scientific attention regarding its initiation and age.

Three sites (named S17, S18 and S20, fig. 2a and 2b) in the Fochteloërveen peat remnant were selected for dating (for further details on choices for site selection see section 2.3). At each of these sites a core containing the mineral-to-peat transition was obtained. Note that the meaning of *basal peat* in this study is much broader than the 'Basisveen Bed' as known in Dutch stratigraphy (TNO-GSN, 2021a). For each of the three sites, selected levels in the peat core were analysed for percentage organic matter (OM) through loss-on-ignition (LOI), plant macrofossils (PM) and testate amoebae (TA). The palaeo-environmental setting was reconstructed based on analyses of PM and TA. Based on LOI data, samples for radiocarbon (^{14}C) dating were selected from multiple levels within each core. When attainable, (charred) plant macrofossils were selected for dating. Additionally the original bulk material was sampled and chemically processed to derive humic and humin fractions for dating. All steps are explained below.

2.2 Study Area

The northern Netherlands was covered by a continental ice sheet during the Saalian (MIS 6), which led to deposition of glacial till (Rappol, 1987; Van den Berg and Beets, 1987; Rappol *et al.*, 1989; TNO-GSN, 2021b) on the Drenthe Plateau or till plateau (Ter Wee, 1972; Bosch, 1990). During the Weichselian (OIS 4-2), aeolian cover sands were deposited over an extensive area of Northwest Europe, forming the European Sand Belt (Koster, 1988, 2005). On the Drenthe Plateau these cover sands occur with a thickness varying from 0.5 to 2 m (Ter Wee, 1979; TNO-GSN, 2021c). The Fochteloërveen peat remnant is located near the western edge of the Drenthe Plateau and is part of three catchments, draining into the rivers Drentsche Aa, Peizerdiep and Tjonger (fig. 2c). Historical data of the 18th century indicate that peat thickness at the Fochteloërveen has diminished over the past centuries with as much as 7 m at some locations (Douwes and Straathof, 2019). Our corings (see section 2.3) demonstrated that peat thickness currently varies from 20 cm to 225 cm at approximately 100 visited locations distributed over the peatland. Current climate is characterised by average temperatures of 2.8° C in

January and 17.5° C in July, average annual rainfall of 805 mm, and a potential evapotranspiration of 566 mm (KNMI, 2021).

As a result of large-scale historical peatland reclamations (e.g. Gerding, 1995; Van Beek *et al.*, 2015) currently only small remnants of the former extensive Northwest European peat landscapes remain (fig. 2d). The Fochteloërveen remnant is protected as Natura 2000 area and harbours a wide range of plant and animal species (Provincie Drenthe, 2016). Main threats to the quality and continuity of the area include atmospheric nitrogen deposition and desiccation due to intense drainage for surrounding agriculture. Since the 1980s nature conservation is aimed at peatland restoration (Straathof et al., 2017).

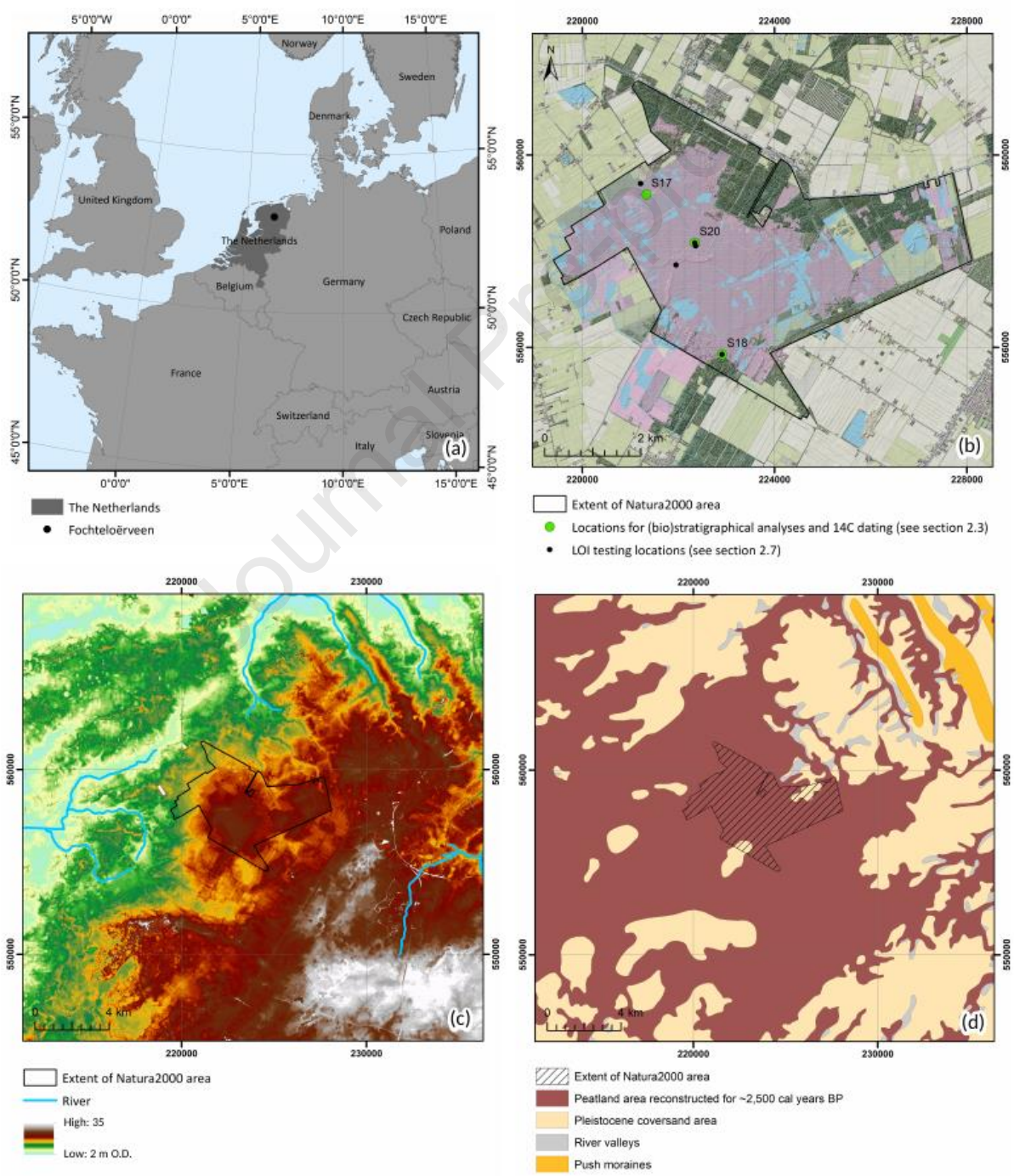

Figure 2. (a) Location of the Netherlands and the Fochteloërveen peat remnant in Europe. (b) Topographical map of Fochteloërveen, indicating sampling locations. Dataframe coordinates are in metres (Dutch RD-new [*Rijksdriehoeksstelsel*] projection). (c) Digital Elevation Model (DEM) of Fochteloërveen and surroundings, showing the main drainage pattern. Elevation is in metres relative to Dutch Ordnance Datum (O.D., roughly mean sea level). (d) Reconstructed palaeogeography for ~2500 cal years BP, indicating assumed former extent of the peatland area around Fochteloërveen. Sources: topography (OpenSimpleTopo, 3200 pixels/km) by Van Aalst (2021); DEM of the Netherlands (AHN3; horizontal resolution 5 m, vertical resolution 0.1 m) from AHN (2021a, 2021b); rivers from Ministerie van Verkeer en Waterstaat (2007); Natura 2000 area from Ministerie van Economische Zaken (2018), palaeogeographical map (500 BC) from Vos and De Vries (2013) and Vos *et al.* (2020).

[2-column fitting figure]

2.3 Site selection and stratigraphy

We performed an elaborate field exploration of the peat remnant consisting of around 100 corings (some grouped in transects of 185 to 575 m long). For each core the stratigraphy was described (see table 2 for details).

As the basal peat is not oligotrophic (see Results for further information), field determination of the degree of humification using the scale for ombrotrophic peat by Von Post (Aaby, 1986) does not fully apply. Additionally, the use of Munsell colour charts for fresh organic deposits is often difficult as the material changes in colour following exposure to oxygen. Instead, we applied a simplified version of the organic-facies determination key by Bos *et al.* (2012), which is originally intended for organic sediments in deltaic settings. Our basic field classification differentiates amorphous organic material (cq. *amorphous organics* in Bos *et al.*, 2012), and non-decomposed peat (cq. *oligotrophic peat* in Bos *et al.*, 2012) where further botanical specification is obtained later through microscopic analyses of plant macrofossils.

Following the field exploration, 21 cores originating from sites distributed over the peatland were collected for future analyses. To address the current research aim, three cores were selected based on a set of criteria considering lithological representativity, spatial distribution and elevation (see table 3 for a comparison of these properties and further details on selection criteria). Each core was collected from a transect along a cover sand ridge that underlies the peat deposits. Site S17 (transect in fig. 3) is located in what is probably a valley or topographic low in the sand landscape underlying the peat deposits, cores S20 and S18 (transects not shown) are located at peat-covered flanks of sand ridges.

[2-column fitting table]

Table 2. Lithology and lithogenetic interpretation of the stratigraphical layers occurring from the surface downwards (modified from Bos *et al.*, 2012).

Lithology	*Symbol*	*Lithogenetic interpretation*
Peat with brown colouring and clearly recognisable plant remains.	V3	Non-decomposed peat
Peat with blackish-brown colouring, greasy consistency and very few recognisable plant remains.	V3*	Amorphous peat (highly humified; *sapric* cf. WRB-IUSS, 2015)

Mixture of peat with very fine to moderately fine sand, dark brown colouring.	ZV/VZ	Peaty sand/sandy peat (gradual transition zone from Pleistocene mineral deposits to overlying organic deposits)
Very fine to moderately fine sand with colour varying from dark brown to light grey, locally loamy, sporadically containing pebbles (ø 1-5 mm).	P	Pleistocene mineral deposits

[2-column fitting table]

Table 3. (a) Criteria for the selection of sites for a vertical dating series, with their respective rationale. (b) Properties of the three sampled sites compared with the minimum (Min), maximum (Max) and average (Avg) of the in total 21 sampled sites of the peat remnant (i.e., where a core for analyses was collected). The surface elevation was measured with a vertical precision of ~10 mm. The total thickness of organic deposits is the sum of V3, V3* and ZV/VZ. The top of the Pleistocene mineral deposits was derived from the surface elevation minus the total thickness of organic deposits as determined visually in the field (i.e., might deviate slightly from the *basal peat* layer that was defined later based on OM%). NA = not applicable. For other stratigraphical abbreviations see explanation in table 2.

(a)	**Selection criteria**	**Rationale**
	The site is part of a coring transect (distance between 185 and 575 m long).	The coring transect provides relevant background information regarding the landscape position of the site.
	The obtained core contains the (visual) mineral-to-peat transition.	Cores containing the mineral-to-peat transition will be most straightforward to analyse and are not compromised by suboptimal sampling conditions.
	For the three selected sites, the cores have V3* layers of varying thickness, and at least one site contains a ZV layer.	Analyses of three sites with a representative thickness range of V3* and presence of a ZV layer will cover the stratigraphical diversity that is present in the study area (see table 3b) and potentially in other regions. This ensures that any methodological recommendations will have a wide applicability.
	The three selected sample sites are well-distributed spatially and of varying elevation.	Our approach should be applicable to different landscape positions.

(b)	**Property**	**S17**	**S18**	**S20**	**Min**	**Max**	**Avg**
	Surface elevation (m. O.D.)	9.308	11.999	10.781	9.31	12.00	10.70
	Total thickness organic deposits (cm)	216	30	35	30	216	94
	Thickness V3 (cm)	182	16	24	16	182	74
	Thickness V3* (cm)	34	6	11	6	34	17
	Thickness ZV/VZ (cm)	0	8	0	0	8	3
	Top of Pleistocene mineral deposits (m. O.D.)	7.15	11.70	10.26[1]	7.15	11.70	9.70
	Location	East	West	Central	NA	NA	NA

[1] Corrected for standing water at the surface.

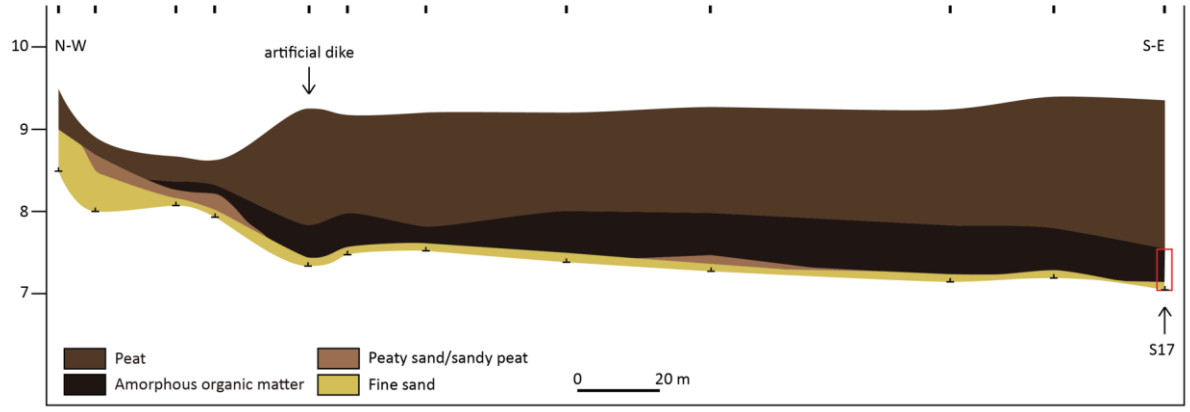

Figure 3. Example cross section, showing stratigraphical context of core S17 (on the right). The red box indicates the sampled reach of the profile. About 1 m further in S-E direction, a wide ditch hampered additional corings to extend the transect. [2-column fitting figure]

Figure 4. Photograph of core S17 taken directly after collecting the core in the field, (a) overview photo (bottom at the right), (b) detail of the mineral-to-peat transition. [2-column fitting figure]

2.4 Collection of cores

The three cores were collected in 2019 with a hand-operated stainless-steel peat corer (Russian type) of 50 cm long and 60 mm outer diameter, with an equivalent core volume of 0.5 dm^3 (Eijkelkamp Soil & Water, 2018). This type of corer was found to be most useful for sampling both peat and water saturated mineral sediments underneath in one core, with minimal disturbance and low risk of contamination. Other types of corers were considered unsuitable for this purpose. For instance, augers or gouge corers often disturb the sample and do not protect it from contamination as there is no closed coring chamber. A Van der Staay suction corer (Wallinga and Van der Staay, 1999), which is used to sample water saturated mineral deposits, cannot sample peat layers as these block the suction mechanism. The Russian corer is generally used for sampling deeper (i.e. mostly catotelm) peat layers (De Vleeschouwer *et al.*, 2010). Field testing demonstrated that this corer was able to simultaneously sample both peat and the top of water saturated mineral deposits adequately (fig. 4). In areas where the mineral deposits are compacted so firmly that hand-operated corers cannot be pressed down to a sufficient depth, the use of percussion drilling equipment might be useful (e.g. Eijkelkamp Agrisearch Equipment, 2022).

Each time prior to sampling a new core, the coring chamber and pivoting blade (fin or lid) were cleaned with a fresh microfiber cloth, followed by a thorough rinse with deionised water. Directly after this cleansing routine the corer was pressed down with the pivoting blade closed. After reaching the desired sampling depth the corer was turned 180° clockwise to collect the sample, upon which the pivoting blade closed the coring chamber and the corer was retrieved. Subsequently the corer was kept horizontally with the pivoting blade facing upwards. The blade was carefully turned to retrieve the (undisturbed) core. At this point the core was photographed. Retrieval and packaging of the core followed the procedures proposed by De Vleeschouwer *et al*. (2010) and Givelet *et al.* (2004), and proceeded as follows. The core was covered with plastic cling film. Then a PVC half-circular pipe was placed over the core, upon which the corer was rotated to transfer the plastic-covered core to the PVC pipe. The exposed side was covered with the remaining plastic film and the core was secured with plastic tape. Through these steps, which took about 5 minutes from retrieval to packaging, handling of the core in the field was minimized. The name, top and bottom of the core were marked with water-resistant labels. The PVC pipes were transported in horizontal orientation to prevent damage to the cores and stored in a refrigerator of 3° C within 12 hours. Location and elevation of all sampling sites were recorded with a Topcon 250 Global Navigation Satellite System (GNSS) receiver, with a horizontal precision of ~5 mm and vertical precision of ~10 mm (RTK; TOPCON, 2017).

2.5 Core processing and subsampling

The cores were opened in the laboratory of BIAX Consult (Zaandam, the Netherlands). Each core was photographed again, the stratigraphy was described and based on visual inspection the approximate mineral-to-peat transition was determined. Around this transition, a range of contiguous 1-cm-thick slices was cut from the core. Outer edges of each slice were carefully cleaned to prevent contamination. Total sample volume for each cleaned level amounted to ~7 cm^3. The samples were subsampled for multi-proxy analysis based on a priority flowchart (fig. 5), which is further explained below.

A bulk subsample (2 cm^3) was collected for dating. The remaining material (around 5 cm^3) was used for PM to analyse plant species and to select suitable plant macrofossils for radiocarbon dating. The PM subsamples were obtained from the filtrate after gently rinsing with warm water over a 0.25 mm sieve. A pollen sample (0.5 ml) was collected from the sieving water for future study and stored at 3° C. Sieving water (0.5 ml) and any remaining non-sieved material (ranging between 1 up to 3 cm^3 depending on how much material remained) was collected for TA analysis. Considering its destructive protocol, LOI was performed only on non-sieved material that remained after TA analysis (typically between 1 and 2 cm^3). To gain more insight in the organic matter gradient in the cores, additional levels were sampled where only LOI was performed (without biostratigraphical analyses and ^{14}C dating). For these levels 2 cm^3 of unsieved material was used for LOI, the remainder was stored at 3° C for future reference. Table 4 provides an overview of all collected subsamples for the three cores.

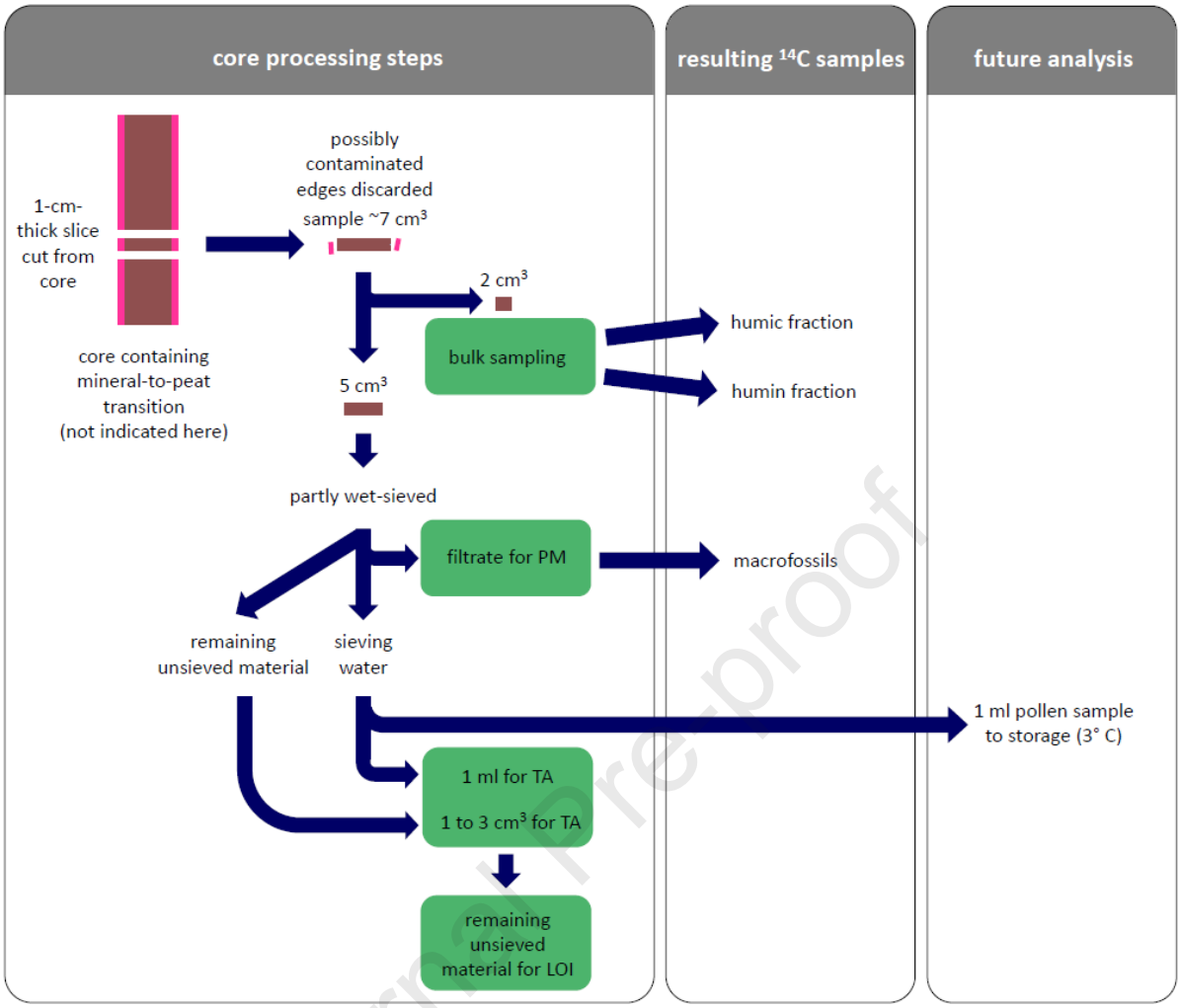

Figure 5. Flowchart showing allocation of sample material from each 1-cm-thick core slice, subsequent processing steps and resulting fractions for ^{14}C dating. PM = plant macrofossil analysis, TA = testate amoebae analysis, LOI = loss-on-ignition. [2-column fitting figure]

346 [2-column fitting table]

347 ***Table 4.*** Overview of analyses and resulting fractions for ^{14}C dating for each investigated level of the cores S17, S18 and S20.

348 PM = plant macrofossil, TA = testate amoebae, LOI = loss-on-ignition.

Core	From (m O.D.)	To (m O.D.)	PM analysis	TA analysis	LOI	^{14}C bulk humic	^{14}C bulk humin	^{14}C macro-fossils
S17	7.495	7.505	X	X		X	X	X
	7.485	7.495	X	X	X	X	X	X
	7.475	7.485	X	X		X	X	X
	7.430	7.440	X		X			
	7.390	7.400	X		X			
	7.350	7.360			X			
	7.300	7.310	X	X	X	X	X	X
	7.290	7.300	X	X	X	X	X	X
	7.280	7.290	X	X		X	X	X
	7.230	7.240			X			
	7.220	7.230			X			
	7.210	7.220	X	X	X	X	X	X
	7.200	7.210	X	X	X	X	X	X
	7.190	7.200	X	X		X	X	X
	7.180	7.190	X	X	X		X	
	7.170	7.180	X	X	X	X	X	
S18	11.80	11.81	X	X	X	X	X	
	11.79	11.80	X	X	X	X	X	X
	11.78	11.79	X	X	X	X	X	X
	11.77	11.78	X	X		X	X	X
	11.76	11.77			X			
	11.75	11.76			X			
	11.74	11.75			X			
	11.73	11.74	X	X		X	X	X
	11.72	11.73	X	X	X	X	X	X
	11.71	11.72	X	X	X	X	X	
	11.70	11.71	X	X		X	X	
	11.69	11.70			X			
	11.68	11.69	X	X		X	X	
	11.67	11.68	X	X	X	X	X	
	11.66	11.67	X	X	X	X	X	
	11.65	11.66	X	X		X	X	
S20	10.40	10.41			X			
	10.39	10.40			X			
	10.38	10.39	X	X	X	X	X	
	10.37	10.38	X	X	X	X	X	X

10.36	10.37	X	X	X	X	X	X
10.35	10.36	X	X	X		X	
10.34	10.35			X			
10.33	10.34	X	X	X	X	X	X
10.32	10.33	X	X	X	X	X	X
10.31	10.32	X	X		X	X	X
10.30	10.31	X	X	X	X	X	
10.29	10.30	X	X		X	X	
10.28	10.29			X			
10.27	10.28			X			
10.26	10.27	X	X		X	X	X
10.25	10.26	X	X	X	X	X	X
10.24	10.25	X	X	X	X	X	X

2.6 (Bio)stratigraphical analyses

The percentage organic matter was determined using LOI (see e.g. Chambers *et al.*, 2011; Kennedy and Woods, 2013). The used subsamples for LOI had a volume of 1 to 2 cm^3. Sample dry weight was determined after drying for 24 hours at 105° C, followed by combustion at 550° C. Subsample dry weight was ~0.65 g on average, of which the remaining mineral component (dry ash) after combustion amounted to ~0.29 g. A microbalance (0.0001 g) was used to maximise measurement precision for these small subsample sizes.

PM analyses were conducted at BIAX Consult in Zaandam, the Netherlands. Mosses and seed remains of vascular plants in the filtrate were identified with a Leica binocular incident light microscope at magnifications of x6 to x50. Identifications followed Körber-Grohne (1964, 1991), Berggren (1969, 1981), Anderberg (1994), Smith (2004), and Cappers *et al.* (2006).

TA subsamples were analysed at Queen's University Belfast, United Kingdom. These subsamples were wet-sieved at 300 µm and back-sieved at 15 µm following standard procedures described by Booth *et al.* (2010). Two slides per sample (2 x 21 x 21 mm cover glasses) were studied using a high power binocular microscope under x20 to x40 magnification.

2.7 Defining basal peat (determining M_d value)

To gain a thorough understanding of the OM gradient around the mineral-to-peat transition in our study area prior to selecting a defining OM value (i.e., M_d, fig. 1b) above which the material is called *peat*, a vertical series of LOI measurements was performed for five duplicate cores (i.e., additional cores that were collected approximately 10 cm next to the locations of the 21 sampling sites). In this way, the OM gradient could be determined for a continuous sequence (of 22 to 26 cm long) with a resolution of 1 cm (note that this was not fully possible for the cores of sites S17, S18 and S20 that were collected for dating, as for some investigated levels no unsieved material remained after completion of the biostratigraphical analyses to perform LOI). The resulting OM gradients were analysed to derive a substantiated value for M_d.

375

376 ***2.8 Radiocarbon dating***

377 The material reserved for bulk sampling was used without removal of roots and provided sufficient humics and
378 humins to date for nearly each level (table 4). For plant macrofossil samples, only charred aboveground plant
379 material was selected for radiocarbon dating; waterlogged (uncharred) belowground plant remains like rootlets,
380 radicelles and rhizomes were present abundantly, but aboveground waterlogged plant remains were scarce.
381 From 22 levels of the three cores, charred aboveground plant remains from terrestrial plants could be retrieved
382 (table 4 and 5).

383 Radiocarbon measurements were performed at the Centre for Isotope Research of the University of
384 Groningen (the Netherlands), using a MICADAS Accelerator Mass Spectrometer (Ionplus AG; Synal *et al.*, 2007).
385 For background information on the principles of radiocarbon dating we refer to e.g. Bayliss *et al.* (2004); Bronk
386 Ramsey (2008a); and Törnqvist *et al.* (2015). For a full description of the (pre-treatment) methods in Groningen
387 we refer to Dee *et al.* (2020). Here we only concisely describe details of chemical pre-treatment and other
388 relevant characteristics of our dating samples.

389 The acid-base-acid (ABA) method was applied to all the charred plant remains, with respective temperatures
390 of 80°, 80° and 20° C. For the humin and humic fractions the bulk sample material was first pre-treated with acid
391 and base, both at 80° C. Then the base solution was kept separate and the humic fraction was obtained by
392 addition of acid (at 20° C). The solid humic fraction was rinsed with decarbonized water to almost neutral pH and
393 dried in an oven at 80° C. The solid material (humin fraction) that remained after the base step was rinsed to
394 neutral pH and then treated with acid (at 20° C), rinsed with decarbonized water to neutral pH and dried in an
395 oven at 80° C. The sample material was not sieved during the entire procedure, to secure that the very small
396 organic particles in the bulk material were retained. Instead, a centrifuge was used to separate the solid and
397 liquid fractions. Some of the humin fraction samples contained a lot of sand and little organic remains, which
398 resulted in a very low carbon yield of the combusted subsample (tables 7-9). Also the obtained humic fraction
399 yields were very low for several samples.

400 After chemical pre-treatment (sub)samples were weighed in tin capsules and combusted to CO_2 in an
401 elemental analyser (IsotubeCube NCS). This analyser is coupled to an Isotope Ratio Mass Spectrometer (Isoprime
402 100) for measurement of $\delta^{13}C$ in the sample material. Resultant CO_2 was graphitized to carbon using hydrogen
403 and an iron catalyst. The graphite was pressed into aluminium cathodes and measured on ^{12}C, ^{13}C and ^{14}C atoms
404 with the MICADAS. The samples measured as graphite in the AMS, can be divided in two groups. Part of the
405 humic and humin fractions were relatively small (up to 1 mg carbon) and these samples were measured in an
406 AMS batch for small-sized samples. The measurement error for these samples is around ±40 yrBP. The other part
407 of the samples was measured as graphite in a regular AMS batch (for masses >1 mg and <2.5 mg C) and the
408 measurement uncertainty for these samples is in general below ±30 yrBP.

409 Three charred plant remains samples of S17 (M6, M12 and M3) and one humic fraction of S18 (M12) had very
410 small sizes (< 0.5 mg) and were treated in a different way. These samples were combusted with an elemental
411 analyser (Isotube Cube) to CO_2. The CO_2 was led into the AMS and measured directly on carbon isotopes. Since
412 much lower carbon masses are measured in the AMS (in a much shorter time period) when introduced as CO_2

gas compared to graphite samples, the measurement uncertainty for these samples is larger (± 60-80 yrBP) compared to the samples measured as graphite.

The ^{14}C measurement results ($F^{14}C$ and ^{14}C age in tables 7-9) are calculated according to the conventions (Stuiver and Polach, 1977), OX-II (SRM 4990C) was used as calibration standard, and the results are corrected for background signals using background reference materials and for isotopic fractionation using the $\delta^{13}C$ value measured with AMS.

2.9 Calibration and age-depth modelling

The radiocarbon dates were calibrated using IntCal20 (Reimer *et al.*, 2020) in the OxCal program (version 4.4, Bronk Ramsey, 1995). The calibrated ages are presented as likelihoods in age-depth plots in OxCal (i.e., initially no further assumptions were applied in a Bayesian modelling framework). Subsequent modelling was based on the following assumptions:

- Plant macrofossil ages provide the best estimate of the age of a peat layer (based on correct chronology as shown in fig. 7a/e/i and in line with the consensus in literature to date short-lived, aboveground plant macrofossils of terrestrial species with AMS, see e.g. Piotrowska et al., 2011).
- For reasons outlined in fig. 1, humic and humin samples may potentially yield different ages than plant macrofossil samples.
- Agreement of humic/humin ages with plant macrofossil ages indicates that the humic/humin samples are contemporaneous with the peat layer from which they were obtained. As such, they provide a representative indication of the age of the peat layer.
- In contrast, disagreement of humic/humin ages with plant macrofossil ages indicates that the humic/humin samples are not contemporaneous with the peat layer from which they were obtained, and do not accurately represent the age of the peat layer.

For each core, the dates of plant macrofossils were modelled using the P_Sequence function (Bronk Ramsey, 2008b) as follows. Start and end of the P_Sequence were defined with a Tau_Boundary and regular Boundary respectively. The levels of the start of the peat initiation process, basal peat layer and end of the peat initiation process (i.e., as based on %OM data, see fig. 7) were specified in the P_Sequence. If no macrofossil date for these levels was available, the Date command was added as query to generate an age distribution. The Difference command was used to calculate a distribution for the amount of time that passed between the start and end of the peat initiation process. A t-type outlier model (Bronk Ramsey, 2009) using a T(5) distribution and U(0,4) scale was combined with the P_Sequence. The t-type outlier model is intended for cases where the measured sample might not relate to the event being dated (Bronk Ramsey, 2009). The prior probability for a macrofossil date to be an outlier was set to 5% (i.e., one out of twenty might be an outlier). The resulting age-depth models were calculated based on a model averaging approach, where macrofossil dates that are more probable to be outliers are down-weighted (Bronk Ramsey, 2009). See the Data Availability Statement for the OxCal scripts.

The likelihoods of humic and humin ages were plotted together with the macrofossil-based P_Sequences. The degree of overlap of the humic/humin likelihoods with the 95% confidence interval of the P_Sequences

450 indicates the accuracy of the humic/humin dates in representing the age of the peat layer from which they were
451 obtained.
452
453
454 [2-column fitting table]
455 ***Table 5.*** Overview of the charred aboveground plant remains that were selected for radiocarbon dating. When a number is
456 given, this is the exact amount encountered, cf. = resembles, + = present, ++ = frequent. The sample weight is the mass of the
457 sample before the start of the chemical pre-treatment.

Core	From (m O.D.)	To (m O.D.)	Aboveground plant remains (all charred) for ^{14}C dating	Sample weight (mg)
S17	7.495	7.505	*Calluna vulgaris*, twig fragments + Herbaceous stem, fragments + *Sphagnum*, stem fragments +	8.63
	7.485	7.495	*Erica tetralix*, leaf fragments + *Calluna vulgaris*, twig fragments + *Calluna/Erica*, twig fragments + Herbaceous stem, fragments + *Bryales*, stem fragments +	20.78
	7.475	7.485	*Erica tetralix*, 3 leaves *Eriophorum vaginatum*, 1 spindle *Calluna/Erica*, twig fragments +	4.21
	7.300	7.310	Deciduous wood, undetermined	1.36
	7.290	7.300	Herbaceous stem fragments +	0.87
	7.280	7.290	Herbaceous stem ~18 fragments (incl. cf. *Juncus*)	11.75
	7.210	7.220	Herbaceous stem fragments (cf. *Eriophorum*) ++	9.70
	7.200	7.210	Herbaceous stem and stem base fragments (cf. *Eriophorum*) ++	12.99
	7.190	7.200	Herbaceous stem ~16 small fragments	3.07
S18	11.79	11.80	*Calluna vulgaris*, twig fragments + *Calluna/Erica*, twig fragments + Herbaceous stem, fragments + *Sphagnum*, stem fragments +	2.34
	11.78	11.79	*Calluna/Erica*, twig fragments + Herbaceous stem, fragments +	0.57
	11.77	11.78	Cyperaceae (cf. *Eriophorum*), stem base 3 fragments Herbaceous stem, fragments +	3.30
	11.73	11.74	*Calluna/Erica*, twig fragments (lower parts) + Herbaceous stem, fragments + *Sphagnum*, stem 1 fragment	8.16
	11.72	11.73	*Calluna/Erica*, twig fragments + Herbaceous stem, fragments +	7.44
S20	10.37	10.38	*Erica tetralix*, 1 leaf	4.98

		Calluna/Erica, twig fragments +	
10.36	10.37	*Erica tetralix*, 2 leaves *Calluna/Erica*, twig fragments +	18.09
10.33	10.34	*Erica tetralix*, 1 leaf *Calluna/Erica*, twig fragments + *Bryales*, stem fragments +	4.86
10.32	10.33	*Calluna/Erica*, twig fragments	5.26
10.31	10.32	*Calluna/Erica*, twig fragments + Herbaceous stem, fragments +	4.47
10.26	10.27	Herbaceous stem, 2 small fragments	0.04
10.25	10.26	Herbaceous stem, fragments + Charcoal, small fragments +	1.58
10.24	10.25	Herbaceous stem, 1 fragment Charcoal, 1 small fragment	1.04

458

459 **3 Results**

460 ***3.1 The organic matter gradient of the mineral-to-peat transition: defining basal peat (M_d)***

461 The five vertical series of LOI measurements to derive the OM gradient at the mineral-to-peat transition are
462 shown in fig. 6. The data show a clear and abrupt rise of OM over a distance of a few cm. Based on this outcome
463 *peat* was defined as material with an OM percentage of 40% or higher (i.e., the defining value M_d = 40%). The
464 layer called *basal peat* is therefore the first cm of material with OM ≥ 40%.

465

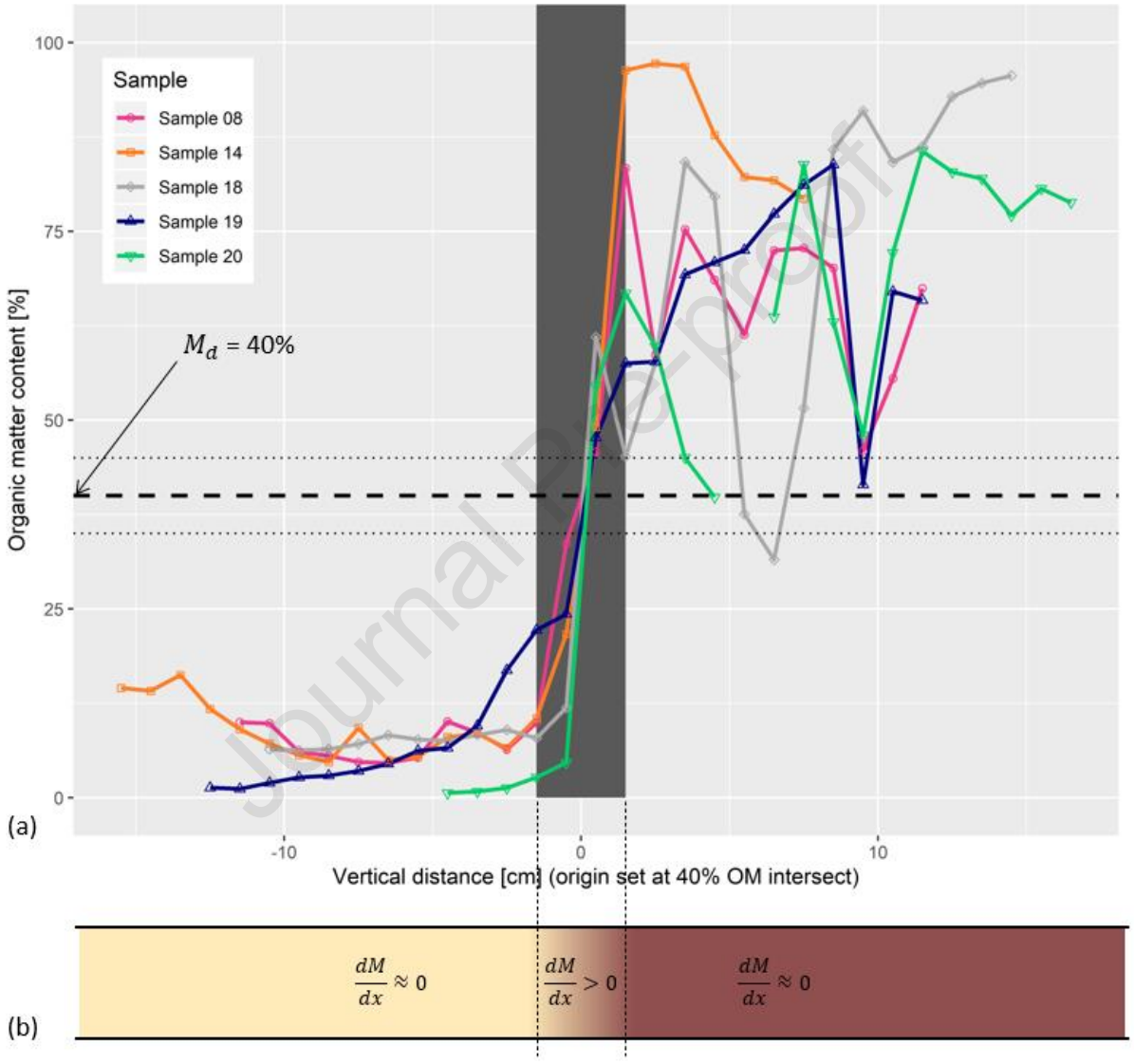

466

467 ***Figure 6.*** (a) Organic matter data of five cores (for locations, see fig. 2). The dashed horizontal line shows the value of M_d,
468 which was set at 40% OM. The dotted horizontal lines indicate an OM content of 35% and 45% for ease of comparison. For
469 one 1-cm-thick layer of core 20 no data were available, this causes the discontinuity in the green line. (b) Schematic core
470 rotated 90° clockwise, showing conceptual organic matter gradient (see also fig. 1b).

471 [2-column fitting figure]

472

473

474

3.2 Plant macrofossils (PM) and testate amoebae (TA)

Overall the samples that originated from the stratigraphical layer described as amorphous organic matter (table 2) contained few macrofossils. In the non-decomposed (waterlogged) peat (table 2) mostly belowground remains such as rootlets, radicelle and rhizomes were preserved. Few waterlogged aboveground plant tissues were present, however charred aboveground remains could often be identified (table 6).

In general, all investigated levels of the three cores contained small unidentifiable rootlets. Part of the rootlets was of Cyperaceous origin, of which some were identified as *Carex* radicelle. The bottom levels of S18 and S20 contained fine sand, and in some of these levels also sclerotia of the mycorrhizal fungus *Cenococcum geophilum* were present. In the core of lowest elevation, S17, the bottom levels (7.17 to 7.20 m O.D.) contained a few leaves of *Sphagnum austinii* (*S. imbricatum*) and six megaspores of *Selaginella selaginoides*. From 7.20 to 7.22 m O.D. many charred herbaceous stems were present, of which some likely derived from stem bases (corm) of *Eriophorum*. Slightly higher in the profile (7.28 to 7.31 m O.D.) fewer herbaceous stems were observed and many sclerotia of the fungus *Cenococcum geophilum* were found. The upper three levels, from 7.475 to 7.505 m O.D., contained vegetative remains of *Eriophorum vaginatum*, *Erica tetralix*, *Calluna vulgaris*, *Bryales* species, *Sphagnum austinii* and other *Sphagnum* species. In core S20, between 10.30 and 10.34 m O.D., leaf and/or stem remains of Poaceae (including *Phragmites* and other species) were present, which were not found in core S17 and S18. In the upper levels of cores S18 and S20, charred herbaceous stems and twigs of *Calluna vulgaris* and/or *Erica tetralix* were found. In addition, the upper levels of core S20 contained some stems of *Bryales* mosses, whereas in core S18 some charred *Sphagnum* stems were found. Both core S18 and S20 contained waterlogged seeds of *Juncus* (*Juncus conglomeratus/effusus*) in their upper levels.

Almost none of the investigated levels contained suitable material for testate amoebae analyses. In four subsamples only a few damaged or broken tests were present, which could be identified as *Difflugia pristis* or other *Difflugia* species.

Table 6. Results of the analyses of plant macrofossils and testate amoebae. When a number is given, this is the exact amount encountered, (c) = charred, cf. = resembles, + = present, ++ = frequent, +++ = abundant, ++++ = extremely abundant, NA = not available. Final column indicates stratigraphy (also see table 2), MtP (indicated with light grey shading) = mineral-to-peat transition (see fig. 7), BP = basal peat.

Core	From (m O.D.)	To (m O.D.)	*Sphagnum*, stem fragments (c)	*Sphagnum austinii*, leaves	*Bryales*, stems (c)	*Calluna vulgaris*, twig fragments (c)	*Calluna vulgaris*, leaves (c)	*Calluna vulgaris*, leaves	*Calluna/Erica*, twig fragments (c)	*Erica tetralix*, leaves, fragments (c)	*Erica tetralix*, leaves, fragments	Poaceae (excl. *Phragmites*), leaf/stem epidermis	Poaceae (incl. *Phragmites*), leaf/stem epidermis	*Eriophorum vaginatum*, spindle (c)	Cyperaceae, cf. *Eriophorum*, stem base (c)	Herbaceous stem fragments (c)	*Juncus*, seeds	*Juncus conglomeratus/effusus*, seeds	*Carex*, radicelle	Cyperaceae, rootlets/radicelle	Undetermined rootlets/radicelle	Undetermined rhizome epidermis	Wood, decidous, fragments (c)	*Cenococcum geophilum*, sclerotia	*Selaginella selaginoides*, megaspores	*Difflugia*	*Difflugia pristis*	Charcoal, fragments	Fine sand	Stratigraphy
17	7.495	7.505	+	+		+										+					+++	+								peat
17	7.485	7.495		+	+	+		2	+	+						+					+	+								peat
17	7.475	7.485							+	3				1							+++									peat
	||	||																											
17	7.430	7.440				8	2			12	1															NA	NA			
	||	||																											
17	7.390	7.400			+											+	+							+		NA	NA			peat
	||	||																											
17	7.300	7.310																		+	+	++	+	++++						peat
17	7.290	7.300														+				+	+++	+++		+++						peat
17	7.280	7.290														18						+		++						peat
	||	||																												
17	7.210	7.220													+	++			+	+	+	+								MtP
17	7.200	7.210													+	++			+	+	+	+								BP
17	7.190	7.200		+												16			+	+	+	+								MtP
17	7.180	7.190																	+	+	+	+								MtP
17	7.170	7.180		+															+	+	+				6		2			MtP
18	11.79	11.80	+			+			+							+		++	+	+	+									peat
18	11.78	11.79							+							+		++	+	+	+									MtP
18	11.77	11.78													3	+		++	+	+	+									MtP
	||	||																											
18	11.73	11.74	+						+							+			+	+	+					1				BP
18	11.72	11.73							+							+			+	+	+								+	MtP
18	11.71	11.72																	+	+	+								+	mineral
18	11.70	11.71																	+	++	++			+					+	mineral
	||	||																											
18	11.68	11.69																	+	++	++			+						mineral
18	11.67	11.68																	+	+	+								+++	mineral
18	11.66	11.67																	+	+	+								+++	mineral
18	11.65	11.66																	+	++	++			+					+++	mineral
20	10.37	10.38							+	1								++		++	+									peat
20	10.36	10.37							+	2									+	+	++									peat
	||	||																											
20	10.33	10.34			+				+	1			+							+	++	+								MtP
20	10.32	10.33							+											+	++	+								MtP
20	10.31	10.32							+							+				+	++	+								MtP
20	10.30	10.31										+							+	+	++									BP
20	10.29	10.30																		+	++					1				MtP
	||	||																											
20	10.26	10.27														2			+	+	++								++	mineral
20	10.25	10.26														+				+	++			++				+	++	mineral
20	10.24	10.25														1			+	+	++							1	++	mineral

3.2 Dating results

The radiocarbon dating results for the investigated levels for each core are shown in tables 7 to 9. The calibrated ages, modelled P_Sequences, and OM content are shown in fig. 7. Overall, the chronological order of the dates from macrofossils concurs with stratigraphical position (older at the bottom and younger towards the top). However, there is one reversal in core S20 at 10.31 to 10.32 m O.D.. The chronological order of the humic dates is also largely correct, with a few exceptions of minor reversals (S17: 7.19 and 7.28 m O.D.; S18: 11.65 m. O.D.; S20: 10.24 m. O.D.). For higher levels (above the mineral-to-peat transition), humin ages converge with those based on humics and plant macrofossils. For lower levels however, humin ages are scattered.

Dates of plant macrofossils, humics and humins diverge for samples from the mineral-to-peat transition (i.e., in fig. 7 between 'Start of peat initiation process' and 'End of peat initiation process'), especially for core S17. The higher in the profile and the further away from the mineral-to-peat transition, dates of plant macrofossils and both humic and humin fractions are increasingly in agreement. At the levels where the radiocarbon ages diverge, dates of plant macrofossils represent the oldest fraction in cores S17 and S18. For core S17 the difference between the macrofossils and humics is relatively constant for the samples below 7.22 m O.D., while also the dates of these fractions are relatively constant with increasing depth. In core S20, no plant macrofossils were available from the sandy layers at the bottom. Here, the humics are generally oldest, humin ages are very dispersed.

The part of the stratigraphy with the rising OM gradient ('period of peat initiation' as explained in fig. 1b, also see fig. 6) reflects the timespan (duration) of the peat initiation process. Based on the P_Sequences presented in fig. 7, this timespan was modelled (fig. 8). Results show that the peat initiation process took a median of 1073 years at the location of core S17 (91 - 2706 years at 95.4% probability). At the site of S20 the process took a bit longer with a median duration of 1343 years (472 - 2040 at 95.4%). The process took longest at site S18, here the median lies at 1510 years (1301 - 1714 years at 95.4%).

528 [2-column fitting table]

529 ***Table 7.*** Dating results for core S17. CPR = charred plant remains, NA = not available.

From (m O.D.)	To (m O.D.)	Sample name	Dated fraction	Lab-ID	$F^{14}C$	± (1σ)	^{14}C age (yrBP)	± (1σ)	$\delta^{13}C$ (IRMS)	± (1σ)	%C
7.495	7.505	S17-M9-B	humin	GrM-23376	0.5775	0.0019	4410	26	-27.09	0.15	62.1
7.485	7.495	S17-M8-B	humin	GrM-23797	0.5759	0.0018	4433	26	-27.17	0.15	55.0
7.475	7.485	S17-M7-B	humin	GrM-23515	0.5354	0.0017	5019	26	-27.62	0.15	64.5
7.300	7.310	S17-M6-B	humin	GrM-23516	0.4345	0.0015	6696	29	-27.56	0.15	63.7
7.290	7.300	S17-M5-B	humin	GrM-23517	0.4504	0.0016	6407	29	-28.57	0.15	55.5
7.280	7.290	S17-M4-B	humin	GrM-23520	0.4255	0.0016	6864	30	-27.79	0.15	56.3
7.210	7.220	S17-M12-B	humin	GrM-23731	0.4973	0.0017	5612	27	-28.28	0.15	13.9
7.200	7.210	S17-M11-B	humin	GrM-23732	0.4817	0.0017	5868	29	-28.08	0.15	5.9
7.190	7.200	S17-M3-B	humin	GrM-23733	0.4247	0.0016	6878	30	-28.25	0.15	9.5
7.180	7.190	S17-M2-B	humin	GrM-23734	0.4644	0.0017	6162	29	-28.05	0.15	10.7
7.170	7.180	S17-M1-B	humin	GrM-23736	0.5023	0.0017	5532	27	-28.16	0.15	7.2
7.495	7.505	S17-M9-B	humic	GrM-23285	0.5821	0.0019	4346	26	-28.13	0.15	57.2
7.485	7.495	S17-M8-B	humic	GrM-23829	0.5759	0.0019	4433	27	-27.09	0.15	50.5
7.475	7.485	S17-M7-B	humic	GrM-23830	0.5477	0.0018	4836	27	-28.45	0.15	49.1
7.300	7.310	S17-M6-B	humic	GrM-23831	0.4527	0.0016	6365	30	-28.23	0.15	50.3
7.290	7.300	S17-M5-B	humic	GrM-23832	0.4486	0.0016	6439	29	-28.45	0.15	56.8
7.280	7.290	S17-M4-B	humic	GrM-24024	0.4585	0.0016	6264	29	-27.49	0.15	9.3
7.210	7.220	S17-M12-B	humic	GrM-24025	0.4408	0.0016	6580	29	-26.79	0.15	15.7
7.200	7.210	S17-M11-B	humic	GrM-23865	0.4346	0.0016	6695	30	-26.99	0.15	20.9
7.190	7.200	S17-M3-B	humic	GrM-23866	0.4465	0.0016	6477	30	-27.30	0.15	15.0
7.170	7.180	S17-M1-B	humic	GrM-23867	0.4383	0.0016	6625	30	-27.57	0.15	22.1
7.495	7.505	S17-M9	CPR	GrM-23521	0.5791	0.0017	4388	24	-26.32	0.15	66.1
7.485	7.495	S17-M8	CPR	GrM-23522	0.5786	0.0019	4395	26	-26.55	0.15	61.5
7.475	7.485	S17-M7	CPR	GrM-23523	0.5315	0.0018	5077	27	-27.85	0.15	67.1
7.300	7.310	S17-M6	CPR	GrM-23491	0.4032	0.0041	7300	80	NA	NA	NA
7.280	7.290	S17-M4	CPR	GrM-23524	0.4097	0.0016	7168	30	-26.30	0.15	64.0
7.210	7.220	S17-M12	CPR	GrM-23492	0.3513	0.0033	8400	80	NA	NA	NA
7.200	7.210	S17-M11	CPR	GrM-23525	0.3556	0.0013	8305	30	-25.42	0.15	63.1
7.190	7.200	S17-M3	CPR	GrM-23493	0.3528	0.0036	8370	80	NA	NA	NA

530

531

532

533 [2-column fitting table]

534 ***Table 8.*** Dating results for core S18. CPR = charred plant remains, NA = not available.

From (m O.D.)	To (m O.D.)	Sample name	Dated fraction	Lab-ID	$F^{14}C$	± (1σ)	^{14}C age (yrBP)	± (1σ)	$\delta^{13}C$ (IRMS)	± (1σ)	%C
11.80	11.81	S18-M12-B	humin	GrM-23819	0.8017	0.0022	1775	22	-27.79	0.15	49.9
11.79	11.80	S18-M11-B	humin	GrM-23820	0.7969	0.0021	1823	22	-28.20	0.15	24.4
11.78	11.79	S18-M10-B	humin	GrM-23822	0.7979	0.0022	1814	22	-28.13	0.15	42.9
11.77	11.78	S18-M9-B	humin	GrM-23825	0.7971	0.0028	1821	29	-27.74	0.15	38.0
11.73	11.74	S18-M8-B	humin	GrM-23826	0.6973	0.0022	2896	26	-27.30	0.15	20.1
11.72	11.73	S18-M7-B	humin	GrM-24009	0.8177	0.0044	1615	45	NA	NA	1.4
11.71	11.72	S18-M6-B	humin	GrM-24010	0.9203	0.0049	665	45	NA	NA	2.8
11.70	11.71	S18-M5-B	humin	GrM-24011	0.5993	0.0035	4115	45	NA	NA	2.8
11.68	11.69	S18-M4-B	humin	GrM-24012	0.6145	0.0033	3910	45	NA	NA	0.08
11.67	11.68	S18-M3-B	humin	GrM-24013	0.5070	0.0028	5455	45	NA	NA	2.4
11.66	11.67	S18-M2-B	humin	GrM-24014	0.6602	0.0036	3335	45	NA	NA	0.05
11.65	11.66	S18-M1-B	humin	GrM-24015	0.8293	0.0048	1505	45	NA	NA	0.05
11.80	11.81	S18-M12-B	humic	GrM-23499	0.7958	0.0064	1840	60	NA	NA	NA
11.79	11.80	S18-M11-B	humic	GrM-23868	0.7963	0.0021	1830	21	-27.91	0.15	49.0
11.78	11.79	S18-M10-B	humic	GrM-23870	0.7938	0.0020	1855	21	-28.22	0.15	53.4
11.77	11.78	S18-M9-B	humic	GrM-23871	0.7790	0.0021	2006	22	-28.66	0.15	53.2
11.73	11.74	S18-M8-B	humic	GrM-23872	0.7117	0.0019	2732	22	-28.35	0.15	49.1
11.72	11.73	S18-M7-B	humic	GrM-23873	0.6861	0.0021	3026	24	-28.31	0.15	38.2
11.71	11.72	S18-M6-B	humic	GrM-23875	0.6029	0.0019	4064	26	-28.04	0.15	36.6
11.70	11.71	S18-M5-B	humic	GrM-23878	0.5718	0.0019	4491	26	-28.31	0.15	36.3
11.68	11.69	S18-M4-B	humic	GrM-23879	0.5526	0.0018	4765	26	-28.93	0.15	39.8
11.67	11.68	S18-M3-B	humic	GrM-23880	0.5410	0.0018	4935	27	-28.91	0.15	37.9
11.66	11.67	S18-M2-B	humic	GrM-23881	0.5380	0.0018	4980	27	-29.06	0.15	32.0
11.65	11.66	S18-M1-B	humic	GrM-23882	0.5512	0.0018	4785	26	-29.16	0.15	28.5
11.79	11.80	S18-M11	CPR	GrM-23287	0.7902	0.0024	1892	24	-28.18	0.15	62.9
11.73	11.74	S18-M8	CPR	GrM-23827	0.6863	0.0020	3024	24	-27.69	0.15	64.0
11.72	11.73	S18-M7	CPR	GrM-23828	0.6659	0.0020	3267	24	-27.62	0.15	62.2

535

536

537 [2-column fitting table]

538 ***Table 9.*** Dating results for core S20. CPR = charred plant remains, NA = not available.

From (m O.D.)	To (m O.D.)	Sample name	Dated fraction	Lab-ID	F14C	± (1σ)	^{14}C age (BP)	± (1σ)	δ^{13}C (IRMS)	± (1σ)	%C
10.38	10.39	S20-M10-B	humin	GrM-23798	0.7686	0.0043	2115	45	-28.06	0.15	49.1
10.37	10.38	S20-M9-B	humin	GrM-23799	0.7692	0.0023	2108	24	-28.55	0.15	47.2
10.36	10.37	S20-M8-B	humin	GrM-23800	0.7693	0.0023	2107	24	-27.04	0.15	27.8
10.35	10.36	S20-M7-B	humin	GrM-23801	0.7423	0.0022	2394	24	-28.10	0.15	37.5
10.33	10.34	S20-M12-B	humin	GrM-23802	0.7131	0.0024	2716	27	-29.16	0.15	16.2
10.32	10.33	S20-M11-B	humin	GrM-23803	0.6628	0.0020	3304	24	-28.60	0.15	26.7
10.31	10.32	S20-M6-B	humin	GrM-23812	0.6608	0.0020	3328	24	-29.69	0.15	29.5
10.30	10.31	S20-M5-B	humin	GrM-23813	0.6518	0.0021	3438	26	-30.09	0.15	34.9
10.29	10.30	S20-M4-B	humin	GrM-24006	0.7512	0.0022	2298	24	NA	NA	7.7
10.26	10.27	S20-M3-B	humin	GrM-24007	0.7451	0.0043	2365	45	NA	NA	2.4
10.25	10.26	S20-M2-B	humin	GrM-23737	0.6413	0.0033	3570	40	NA	NA	13.2
10.24	10.25	S20-M1-B	humin	GrM-24008	0.7963	0.0040	1830	40	NA	NA	1.3
10.38	10.39	S20-M10-B	humic	GrM-23968	0.7723	0.0021	2076	22	-28.07	0.15	53.4
10.37	10.38	S20-M9-B	humic	GrM-24018	0.7707	0.0025	2093	26	-27.94	0.15	42.8
10.36	10.37	S20-M8-B	humic	GrM-24017	0.7543	0.0026	2265	27	-26.83	0.15	16.6
10.33	10.34	S20-M12-B	humic	GrM-23883	0.6954	0.0021	2918	24	-28.05	0.15	35.1
10.32	10.33	S20-M11-B	humic	GrM-24019	0.6635	0.0025	3295	30	-28.20	0.15	27.8
10.31	10.32	S20-M6-B	humic	GrM-23884	0.6530	0.0021	3424	26	-28.22	0.15	49.1
10.30	10.31	S20-M5-B	humic	GrM-24021	0.6419	0.0022	3561	27	-28.77	0.15	46.7
10.29	10.30	S20-M4-B	humic	GrM-23969	0.6473	0.0033	3495	40	-29.29	0.15	32.7
10.26	10.27	S20-M3-B	humic	GrM-23885	0.6247	0.0020	3779	26	-29.11	0.15	30.0
10.25	10.26	S20-M2-B	humic	GrM-24022	0.6135	0.0020	3924	27	-28.75	0.15	14.9
10.24	10.25	S20-M1-B	humic	GrM-23886	0.6290	0.0023	3725	29	-28.85	0.15	20.2
10.37	10.38	S20-M9	CPR	GrM-23814	0.7580	0.0020	2225	22	-24.54	0.15	66.4
10.36	10.37	S20-M8	CPR	GrM-23815	0.7577	0.0020	2229	22	-25.24	0.15	63.9
10.33	10.34	S20-M12	CPR	GrM-23208	0.6962	0.0027	2910	30	-26.94	0.15	60.6
10.32	10.33	S20-M11	CPR	GrM-23817	0.6746	0.0022	3163	26	-26.90	0.15	71.3
10.31	10.32	S20-M6	CPR	GrM-23818	0.6906	0.0021	2974	24	-26.53	0.15	63.1

539

540

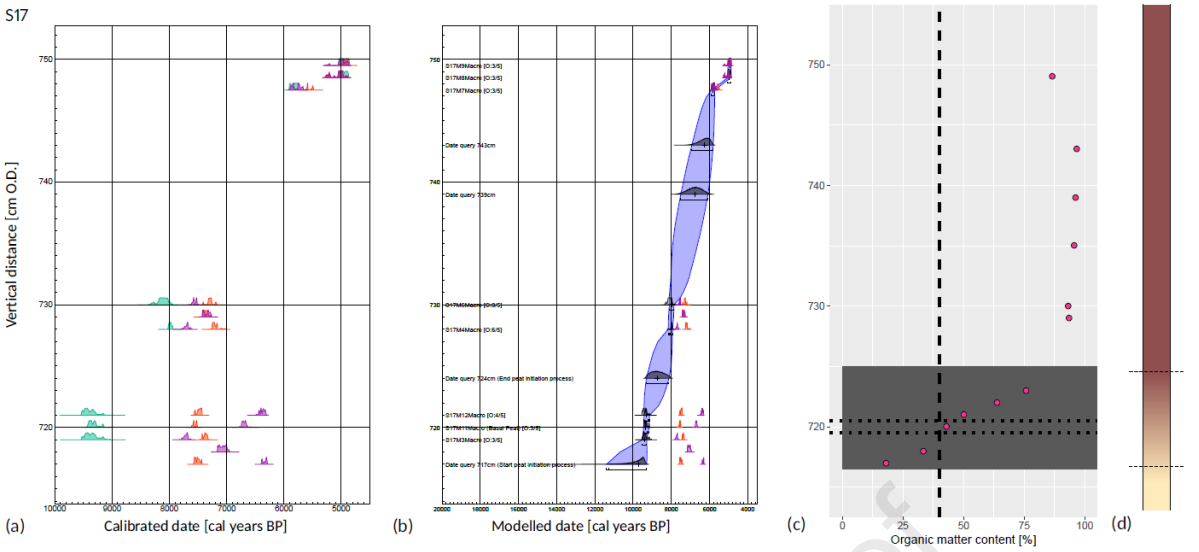

541

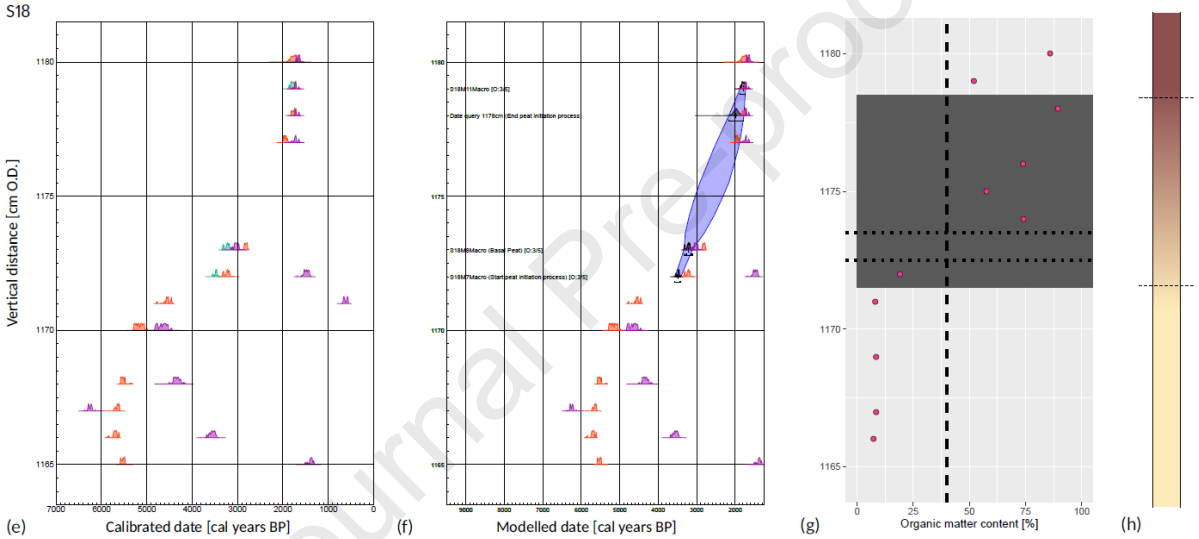

542

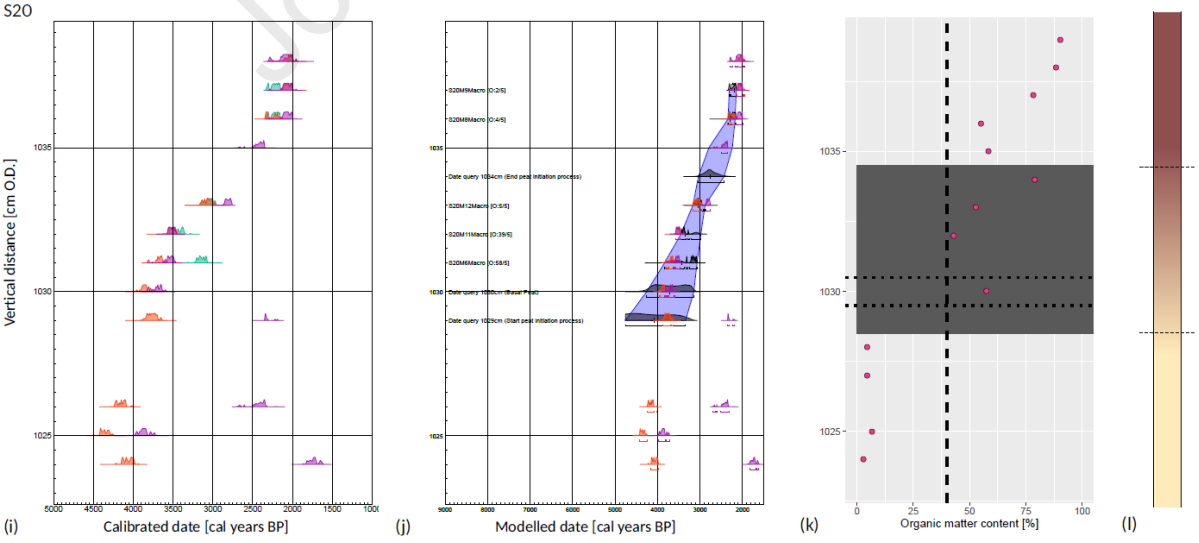

543

Figure 7. Overview of dating results and OM percentages for core S17 (a-d), S18 (e-h) and S20 (i-l). (a/e/i) Age-depth plot showing the likelihoods of all dated fractions; green = macrofossils, orange = humics, pink = humins. Note that some likelihoods overlap, see tables 7-9 for an overview of all dated fractions per layer. (b/f/j) Age-depth plot showing the result of a P_Sequence based on macrofossil dates, accompanied with an outlier model (see Methods for details). The probability for a date to be an outlier is indicated behind each date at the left side of the plot in the format [O:x/5], where x gives the posterior probability and 5 the prior probability that was entered in the outlier model (always set to 5%). Blue shading = 95.4% confidence interval,, + = median of modelled posterior distribution, orange = likelihood of humics, pink = likelihood of humins. Degree of overlap of the humic/humin likelihoods with the confidence interval of the P_sequence indicates accuracy of the humic/humin dates in representing the age of the peat layer from which they were obtained. (c/g/k) Organic matter data, the combination of dashed and dotted lines indicates which sample is the first with OM ≥40%, dark grey shading = samples that encompass the peat initiation process (mineral-to-peat transition). (d/h/l) Schematic cores showing conceptual stratigraphy as in fig. 1b and 6b.

[2-column fitting figure]

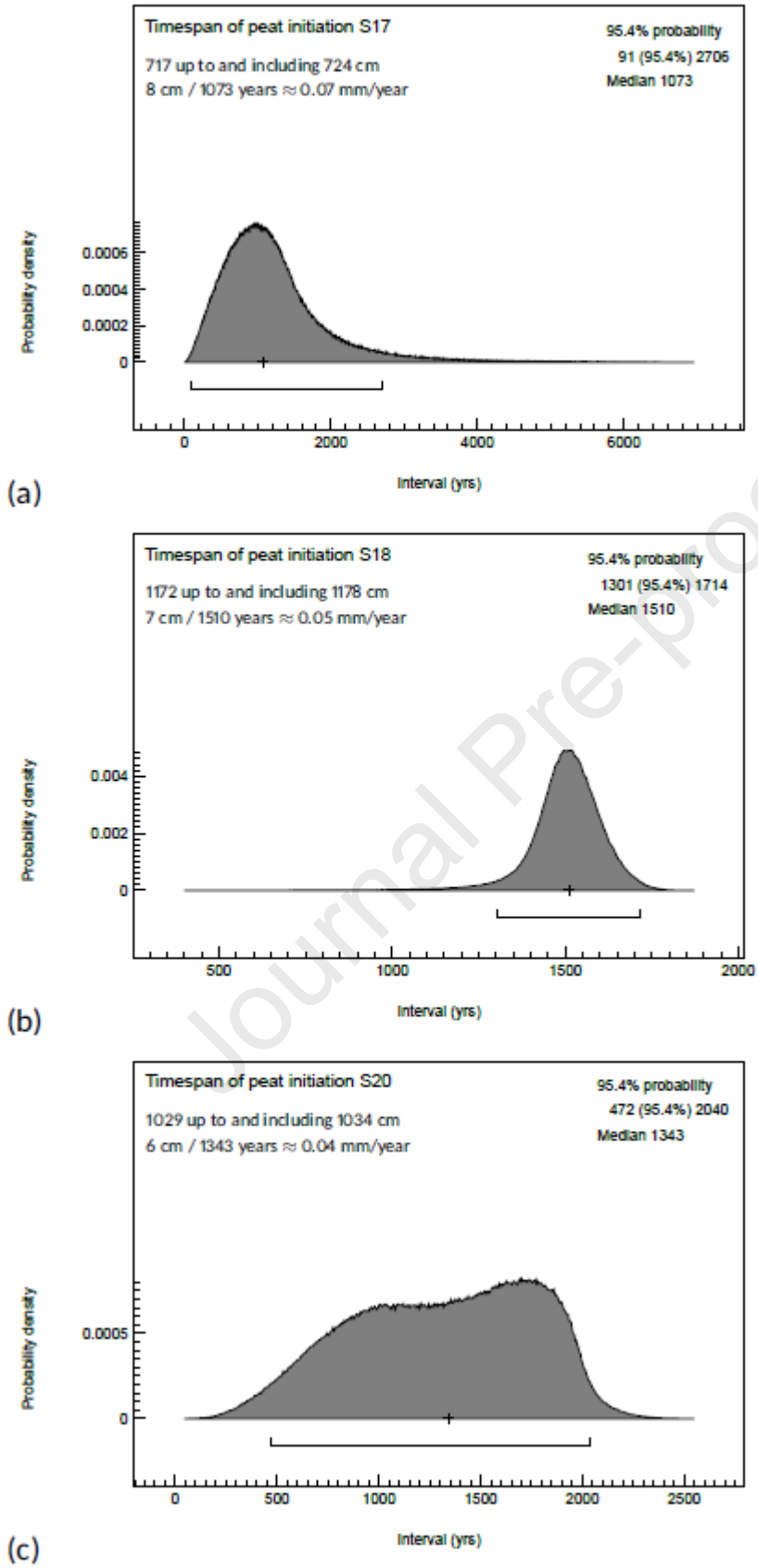

559

560 ***Figure 8.*** Timespan (duration in years) of the peat initiation process in cores S17, S18 and S20, derived from the P_Sequence
561 models shown in fig. 7(b/f/j) (see Methods for details). Apparent accumulation rate (expressed in mm/year) was calculated

562 by dividing the stratigraphical distance of the peat initiation process (provided in cm, see also fig. 7(b/f/j)) by the modelled
563 median of the timespan. Note that these accumulation rates are based on an age-depth relationship (instead of a mass-age
564 relationship) and do not consider gross accumulation and subsequent decay separately, but only the apparent vertical
565 increase (potentially affected by decomposition and/or compaction).
566 [1-column fitting figure]
567

4 Discussion

Here we discuss the process of peat initiation as reflected by the mineral-to-peat transition in the stratigraphical record, the resulting definition of *basal peat* (4.1), followed by the reconstructed palaeoenvironment (4.2), the course and timespan of peat initiation (4.3), and the age assemblage of the different carbon fractions (4.4). Based on this, recommendations for dating *basal peat* are formulated (4.5).

4.1 Mineral-to-peat transition and basal peat (defining M_d)

Our analyses demonstrate that the organic matter content shows a clear and steep rise over a distance of a few centimetres, starting at low values of about 10% and increasing to more than 90% (fig. 6). This gradient reflects the stratigraphical mineral-to-peat transition. The drastic rise in OM content occurs around an OM percentage of 40%. In the explanation of the Dutch soil classification system by De Bakker and Schelling (1966), a range of organic matter classes is defined based on OM and clay percentages (by mass). For soils containing 0 to 8% clay (as in our case study area), the material is called *peat* when containing >35% OM (in case of 8% clay) or >40% OM (when containing 0% clay). This is in strong agreement with the results of our LOI tests (fig. 6), based on which we have selected 40% OM as cut-off value (M_d) above which we define the material as *peat*. The first 1-cm-thick subsample that contained ≥40% OM is therefore defined as the *basal peat* layer.

4.2 Palaeoenvironment

The investigated cores contained a limited amount of well-preserved plant macrofossils. Part of these remains is charred (table 6). In several levels sclerotia of *Cenococcum geophilum*, a mycorrhizal fungus that usually lives in the sandy subsoil, were observed (table 6). In peat, the presence of *C. geophilum* may indicate relatively dry conditions (Van Geel, 1978). Presence of charred and uncharred plant remains in multiple levels of the cores suggests (local) wildfires (for more information on (palaeo)wildfires in peatlands see e.g. Zaccone *et al.*, 2014; Nelson *et al.*, 2021; Rein and Huang, 2021). Dry periods allow further breakdown of material, which could explain the rather poor preservation of uncharred (waterlogged) macrofossils.

It is important to note that even though a bog remnant is studied here, the *basal peat* is in fact fen peat (which is quite often the case; see e.g. Korhola, 1994; Cubizolle *et al.*, 2007). The mineral-to-peat transition is later followed by a fen-bog transition as a result of ombrotrophication (for more information on the latter transition see e.g. Almquist-Jacobson and Foster, 1995; Hughes, 2000; Hughes and Barber, 2004; Väliranta *et al.*, 2017; Loisel and Bunsen, 2020). Our findings indicate that at all three cored locations the peat-forming vegetation was initially mesotrophic. The local vegetation was dominated by sedges, with some presence of *Juncus* (table 6). After the peat initiation process, conditions became more oligotrophic, and the vegetation at S17 and S18 developed probably to an oligotrophic bog with *Calluna vulgaris*, *Erica tetralix* and *Sphagnum* (ombrotrophic conditions). At the location of S20 no *Sphagnum* remains were found, but the vegetation likely changed to a moss (*Bryales*) and heather vegetation.

The investigated cores appeared to be very low in testate amoebae content. However, the presence of *Difflugia* species in a few samples suggests very wet conditions. This taxon and the presence of abundant diatoms (which were observed during TA analysis but not subject of further study) suggest a fen environment (rather than

606 an ombrotrophic bog), which is in agreement with the botanical data. Testate amoebae are often poorly
607 preserved under fen-type conditions, possibly due to predation, physical disaggregation or chemical dissolution,
608 or a combination of these (Roe *et al.*, 2002; Swindles and Roe, 2007; Swindles *et al.*, 2020).

609 In the investigated levels, *C. geophilum* does not occur simultaneously with *Difflugia* species. This mutual
610 exclusion suggests respectively drier and wetter conditions that alternated during the timespan of the peat
611 initiation process. Additionally, a detailed study by Sullivan and Booth (2011) has shown that several *Difflugia*
612 species (including *D. pristis*) are able to cope with fairly high levels of short-term variability in environmental
613 conditions at the peat surface. This variability appeared to be higher at locations with loose-growing *Sphagnum*
614 (rather than dense *Sphagnum* cover) or where vegetation was dominated by vascular plants and non-*Sphagnum*
615 bryophytes (Sullivan and Booth, 2011). We suggest that such conditions may be similar to those in our study area
616 during peat initiation and the transition to an oligotrophic bog.
617
618 ***4.3 Time span of the peat initiation process***
619 The stratigraphical reach with the rising OM gradient (fig. 1b and 6) reflects the timespan of the peat initiation
620 process. Based on the P_Sequences in fig. 7, these timespans were modelled for each core (fig. 8). Results show
621 that this process lasted for 1073, 1510 and 1343 years (medians) for core S17, S18, and S20 respectively. In the
622 stratigraphy, this is reflected in a vertical distance of respectively 8, 7 and 6 cm. This means that apparent vertical
623 accumulation during these first stages of peat development varied between the sites with values of 0.07, 0.05
624 and 0.04 mm/year for core S17, S18, and S20 respectively. A typical value given for the apparent peat
625 accumulation rate in the catotelm is 1 mm/year, and may be lower further down in the catotelm due to
626 compaction and anaerobic decomposition (Rydin and Jeglum, 2013c). A low apparent accumulation rate is indeed
627 the case here, with rates far below 1 mm/year. This implies that 1 cm of peat, at the slowest rate of 0.04
628 mm/year, reflects about 250 years of peat growth.

629 Very few studies have investigated the timespan that is reflected in the first centimetres above the layer they
630 define as *basal peat*. For two cores, Berendsen *et al.* (2007) dated a pair of vertically spaced samples (taken 11
631 cm apart in one core and 9 cm apart in the other), and found age differences of respectively 60 and 120 calendar
632 years. Based on this, they conclude that within-core sampling resolution is less critical than previously assumed.

633 The difference between our results and those of Berendsen *et al.* (2007) highlights that the peat initiation
634 process cannot be assumed to be rapid in all cases and is influenced by environmental setting. Depending on the
635 timespan of the peat initiation process and the apparent accumulation rate, a high vertical sampling resolution
636 and small sample thickness can be crucial to obtain accurate dates. The duration of peat initiation also
637 determines to which degree a date of *basal peat* is representative to use as starting point for build-up of peat
638 deposits.

639 It is important to note that the reconstructed timespans and apparent accumulation rates are based on age-
640 depth relationships (instead of a mass-age relationship). These age-depth relationships do not consider gross
641 accumulation and subsequent decay separately, but only the apparent vertical increase (potentially affected by
642 decomposition and/or compaction). Due to water-saturated conditions for significant periods of time,
643 bioturbation by soil fauna is presumably low during the peat initiation process. This assumption is corroborated

644 by the intact chronostratigraphy of macrofossils shown in our cores (fig. 7a/e/i). As the timespan of the peat
645 initiation process is potentially long, we emphasize that sampling resolution and sample thickness are key points
646 to consider when dating the start of peat growth.
647
648 ***4.4 Age assemblage of carbon fractions***
649 Our data demonstrate that macrofossils (i.e., *in situ* material) in the *basal peat* layer are oldest, and that both
650 humics and humins generally show younger ages. In line with the general consensus in literature (e.g. Piotrowska
651 *et al.*, 2011), we consider the macrofossils to reflect the 'true' age, i.e. representative for the timing when the
652 vegetation accumulated at the specific location. Aboveground remains (no roots) of terrestrial plants are
653 expected to have been in equilibrium with atmospheric ^{14}C values until they died and we therefore do not expect
654 any reservoir effect (also see Blaauw *et al.*, 2004). In this study, samples were carefully selected, cleaned and
655 pre-treated with the full ABA-protocol to minimise the presence of any contamination with carbon from sources
656 other than the original plant materials (see sections 2.6 and 2.8). The macrofossils show a clear chronological
657 order, with samples dating younger upwards in the profile, which suggests that macrofossil relocation through
658 bioturbation is unlikely. There is only one reversal for the macrofossils in core S20 at 10.31 m O.D., while the
659 humic and humin fractions of this same layer do not show a deviation in chronology. The cause for this deviation
660 remains unclear. The outlier model shows that there is an increased chance that either S20M11macro or
661 S20M6macro is an outlier; through the model averaging approach these dates are corrected in the P_Sequence
662 (fig. 7j).
663 Despite the correct chronological order of the humic dates, the age difference between humics and plant
664 macrofossils in core S17 from 7.19 to 7.30 m O.D. shows that the absolute humic ages are likely too young (fig.
665 7a and 7b). This difference in age ranges from about 1700 to 800 years. The same applies to core S18 at depths
666 11.72 and 11.73 m O.D. (fig. 7e and 7f), with age differences of about 250 to 400 years. This is different in core
667 S20, where two humic samples dated older than macrofossils from the same layer. At 10.31 m O.D., the
668 macrofossil sample deviates from the chronology (see above), which causes a fairly large difference with the
669 humic age of approximately 530 years (fig. 7i and 7j). At 10.32 m O.D. however, where the macrofossil date
670 concurs with chronological order, the humic date is only about 120 years older.
671 The humins, both in the *basal peat* but also below in the Pleistocene deposits, show younger ages than the
672 humics and plant macrofossils, and remarkably little coherence. In the sandy Pleistocene layers the organic
673 matter content was low and sand content high. Separating this small amount of carbon from the sand in the lab
674 appeared to be challenging, resulting in several humin samples with fairly low %C (tables 7 to 9). If some younger
675 material is incorporated here, the influence on the resulting age will be larger due this small sample size. This
676 may account for part of the observed variation.
677 Overall, both the humic and humin fractions derived from the mineral-to-peat transition result in younger
678 ages. Fluctuating water tables during the process of peat initiation (discussed above), might explain the origin of
679 younger carbon in these first peat layers. Changes in hydraulic head may lead to both upward and downward
680 (and also sideward) movement of soluble organic compounds (Waddington and Roulet, 1997). Low water levels
681 specifically allow downward water movement through the profile, potentially transporting mobile humic acids

that contain young carbon to lower levels. As the mobility of humics is pH-dependent (Wüst *et al.*, 2008), the initial mesotrophic conditions allow higher mobility than the more acid, ombrotrophic conditions that follow later in time (see above).

Brock *et al.* (2011) dated humic and humin fractions from three grain sizes obtained through wet-sieving (63-125 µm, 125-250 µm and >250 µm), originating from a 1-cm-thick layer positioned 1 cm below the level they regarded to reflect peat initiation. Their results show that for two of these grain sizes, the humic and humin dates are not significantly different from each other. However, both the dates of the humics and the humins become older with increasing grain size, suggesting that the fine particulate matter may be responsible for younger contaminations in both fractions. In our study, the bulk material was not sieved during the entire pre-treatment procedure, to secure that the very small organic particles in the bulk material were retained. Presence of this fine fraction may be responsible for the observed younger dates of the humics and humins, but does not explain the erratic pattern of the humin dates.

Downgrowth of roots may also cause age differences in bulk samples compared to aboveground plant macrofossils, a problem that appears to be of particular relevance in the case of slowly accumulating (fen) peat (Streif, 1972; Törnqvist *et al.*, 1992) such as encountered here during the peat initiation process. The effect may also depend on the botanical composition of the peat-forming vegetation, as certain species such as *Phragmites* or *Eriophorum vaginatum* (table 6) can produce fairly deep roots (Kohzu *et al.*, 2003; Iversen *et al.*, 2015). As humics and humins result from decomposition, their ages may result partly from in-situ carbon and partly from younger carbon that originated from mobile fulvic and humic acids and roots. Additional dating of separated rootlets at multiple levels slightly above the mineral-to-peat transition may shed more light on the sources of error in the ages of the humics and humins for dating peat initiation.

Holmquist *et al.* (2016), who compared radiocarbon dating results for plant macrofossil and bulk samples obtained from basal peat in circum-arctic peatlands, found no significant difference in ages. Based on this they conclude that evidence for a consistent systematic bias introduced by the incorporation of bulk peat dates in large basal ^{14}C databases from peatlands is lacking. In contrast, the large age difference between dates of plant macrofossils and humic or humin dates (up to ~1700 years between macrofossil and humic ages in our case study peatland, and with even larger differences for humins, fig. 7a and 7e) indicates that studies reusing existing bulk dates of *basal peat* should take great care in data interpretation. Some of these studies, which concentrate on regional or global reconstructions of peat initiation (e.g. Tolonen and Turunen, 1996; Macdonald *et al.*, 2006; Ruppel *et al.*, 2013), have important implications for climate research and carbon budgets. Depending on the sample type obtained from the dated *basal peat* layers, dates are potentially interpreted more safely as terminus-ante-quem dates for peat initiation, or should be subjected to rigorous quality assessment prior to data analysis (Quik *et al.*, 2021).

Higher in the peat profile however, dates of plant macrofossils, humics and humins converge, indicating homogeneity regarding carbon fractions and ages. Some of these dates do not differ significantly, others fall within a (very) short timeframe (fig. 7b, 7f and 7j). We suggest that as water tables started fluctuating less, peat accumulation speed began to increase (compare slope in the P_Sequences, most clearly visible for core S18 in fig. 7f), and conditions became more ombrotrophic (start of *Sphagnum* growth, table 6). As a result, downward

water flow declined and mobility of humics decreased. In line with Törnqvist *et al.* (1992) and Blaauw *et al.* (2004), our findings suggest that when focus is not directed towards the *basal peat*, but to higher layers in the peat profile that are characterised by more stable water tables and higher accumulation rates, one might obtain accurate dates through bulk sampling (both humics and humins).

In the mineral soil horizons, i.e. those with <40% OM, generally no (aboveground) plant remains could be recognised. Samples from the stratigraphical layers peaty sand/sandy peat and Pleistocene deposits (i.e., the palaeosoil that became covered with peat, table 2) could therefore only be radiocarbon dated using the humic and humin fractions. Humic acids are considered to be the most reliable fraction for dating organic matter in soils if no plant remains and (almost) no organic carbon is present (Van der Plicht *et al.*, 2019). Indeed, the humin ages of the Pleistocene layers display poor coherence (fig. 7) with frequent stratigraphical inconsistencies. Humic ages in contrast provide results that are stratigraphically consistent. In core S18 for example (fig. 7e), the four humic samples between 11.65-11.69 m O.D. all date around 5500 cal y BP. This consistency could suggest that these samples represent the slow build-up of organic matter in the sandy soil (i.e., at the time prior to peat growth). Some of the humin dates in the mineral horizons show remarkably young ages, perhaps due to the small amount of total carbon in these samples as mentioned above (tables 7 to 9), and relatively larger quantities of carbon from other carbon sources. Dating soil organic matter in mineral soils is complicated and involves different processes than peat initiation (see e.g. Goh and Molloy, 1978; Van Mourik *et al.*, 1995; Van der Plicht *et al.*, 2019), further study of these dates is therefore beyond the scope of the present study.

4.5 Recommendations for dating peat initiation

Our study highlights that peat initiation is a process rather than an event, which has implications for dating peat initiation and *basal peat*. This process is reflected in the stratigraphy as a gradual boundary between mineral sediments and overlying peat deposits. The mineral-to-peat transition can be characterised using the organic matter gradient ($\frac{dM}{dx}$, fig 1b). The use of biostratigraphical indicators to define *basal peat*, as for instance in the approach used by Törnqvist *et al.* (1998), is not always possible due to limited presence of plant macrofossils and potential lack of testate amoebae. However, if material is present and resources allow, including additional biostratigraphical analyses to characterise the palaeoenvironment of the peat initiation process is valuable.

The layer that is interpreted as *basal peat* should be defined clearly and quantitatively, which ensures reproducibility and eases intercomparison of studies. To move towards a quantitative definition of *basal peat*, a simple parameter such as OM is useful as it is easy to measure at low cost, which enables widespread use. Based on the obtained organic matter gradient ($\frac{dM}{dx}$) that reflects the peat initiation process, a value (M_d) can be chosen for the organic matter percentage above which the material is called *peat*. The first cm that has an OM% equal to or above this value is defined as the *basal peat* layer.

Based on our results, an M_d value of 40% OM would be recommendable to define *basal peat* in areas comparable to our case study peatland. This value agrees very well with the Dutch soil classification (De Bakker and Schelling, 1966), especially given the low clay content of the soils in our study area (table 2). However, for peatlands in other regions or with a different botanical composition near the base, LOI-testing may result in a different value for M_d.

As organic matter measurements using LOI require burning the subsample, care should be taken beforehand to ensure sufficient allocation of sample material to all required analyses. Additionally, it should be kept in mind that post-depositional changes such as downgrowth of roots may change OM content, therefore determining the OM gradient over a reach of several cm is useful to contextualise single measurements. We therefore highly recommend to investigate a stratigraphical range to properly contextualise the mineral-to-peat transition and for selecting an OM value to define the *basal peat*.

An additional advantage of organic matter content determination is that this information may help in estimating chances to obtain sufficient amounts of plant macrofossils for ^{14}C dating from specific layers. For the three cores investigated in this study, nearly all (12 out of 14) of the macrofossil samples for dating originated from layers with an organic matter content of 40% or higher. Most of the dated layers with OM below 40% did not contain sufficient macrofossils for dating and were dated solely using humics and humins. Depending on the organic matter gradient and local conditions, this potentially varies between study regions, but may be taken into account for sample selection.

Depending on the timespan of the peat initiation process and apparent accumulation rate, sampling resolution and sample thickness may affect the accuracy of dates in representing the start of peat growth. If accumulation rates are high, a lower vertical sampling resolution or sample size of several cm's might be adequate, whereas lower accumulation rates may require detailed sampling with small sample sizes depending on the research question to be answered. If the timespan of peat initiation and related apparent accumulation rate are unknown, studies aiming to date *basal peat* with a higher accuracy than several hundred (potentially thousand) years should take great care regarding vertical sampling resolution and sample size, as the assumption of a rapid process is not always valid.

An elaborate dating inventory comparable to the approach of the present study is valuable as it provides detailed information on the peat initiation process and on the accuracy of different carbon fractions for dating. To gain insight in the timespan of peat initiation, and consequently to ensure accurate dates of the peat initiation process and *basal peat*, dating several vertically spaced samples within one core as a preceding test is very useful. If time allows, such a layered or multi-stage approach for dating peat initiation and lateral expansion is recommendable (also see staged approaches for dating as suggested by Bayliss, 2009 and Piotrowska *et al.*, 2011). For instance, after obtaining the OM gradient dating plant macrofossils and humics of three levels dispersed over the mineral-to-peat transition would allow substantiated choices for sampling size and resolution for subsequent spatial dating schemes. These preliminary dates and insights may be used to run simulations in OxCal to evaluate potential outcomes of alternate approaches for more extensive (spatial) sampling and dating. If a multi-stage approach is not possible and only one level of each core is dated without prior tests, assumptions on the timespan of peat initiation and related choices in sampling resolution and sample size should be explicitly discussed.

Our findings show that plant macrofossils provide the most reliable age near the mineral-to-peat transition and the *basal peat* layer, and are therefore recommendable to use for ^{14}C dating. The full ABA pre-treatment of macrofossils lowers the risk of chemical contamination and should be applied when possible. If plant macrofossils are unattainable, either due to poor preservation or limited resources for biostratigraphical analyses, dates of

the humic fraction provide the best alternative regarding chronological order. These dates may however deviate from those of plant macrofossils, and our data show that humics can therefore only provide a terminus-ante-quem for the dated levels. If bulk samples are used, it is important to clearly report which fraction was obtained from the sample and used for dating. If marker layers such as tephra are present, these can be used to correlate sites or even provide independent age control if a date can be obtained for the event.

Above the mineral-to-peat transition, our results indicate that dating results of plant macrofossils, humics and humins converge. This implies that humics and humins might be a useful alternative to plant macrofossils for dating peat layers higher in the profile. Justifying this choice would however require a-priori dating knowledge of the peatland under study, and occasional cross-checks with macrofossil dates to ensure accuracy of results.

If the peatland under study is protected as a nature reserve (i.e., not a peat extraction site or location with an outcrop), digging a trench for sampling all the way down to reach the mineral-to-peat transition creates a large disturbance (and would be severely hampered by practical challenges with water infilling). Coring provides an efficient alternative, even though commonly used coring tools such as the Russian corer have a limited sample volume. This limits the options for dating in combination with multiproxy study at a high resolution (Piotrowska *et al.*, 2011). This combination is possible (e.g. as in our study), but requires careful allocation of material to various analyses and involves dating (very) small samples. If chances for obtaining plant macrofossils are encouraging (e.g. based on OM%), one could choose to sacrifice the bulk subsample intended for dating and process it for plant macrofossil analysis. If the expectation regarding plant macrofossils is low, then keeping a bulk sample would offer the possibility to obtain at least a terminus-ante-quem for peat initiation using the humic fraction extracted from the bulk sample.

Textbox 1. *Summary of recommendations for dating peat initiation.*

summary of recommendations for dating peat initiation

- Study the mineral-to-peat transition using the organic matter gradient, and if resources allow, by including biostratigraphical analyses (see [A] in the textbox figure below);
- Take the timespan of the peat initiation process into account when deciding upon sample size and sampling resolution. A layered or multi-stage approach is useful to gain insights on the duration of peat initiation prior to executing elaborate spatial dating schemes (see [B] and [C]);
- Define *basal peat* based on the organic matter gradient to obtain a low-cost, quantitative and reproducible definition that eases intercomparison of studies (see [D]);
- Regarding which fraction to use for ^{14}C dating basal peat (see [E]), our data show that plant macrofossils provide the most accurate age in the mineral-to-peat transition and are therefore recommendable to use. If these are unattainable, dates of the humic fraction provide the best alternative regarding chronological order, but may deviate significantly from the 'true age'. Our results show that humic dates are best interpreted as terminus-ante-quem dates;
- Potentially limited options for sampling and resulting small sample volumes require detailed consideration of allocating material to analyses (see fig. 5 for an example).

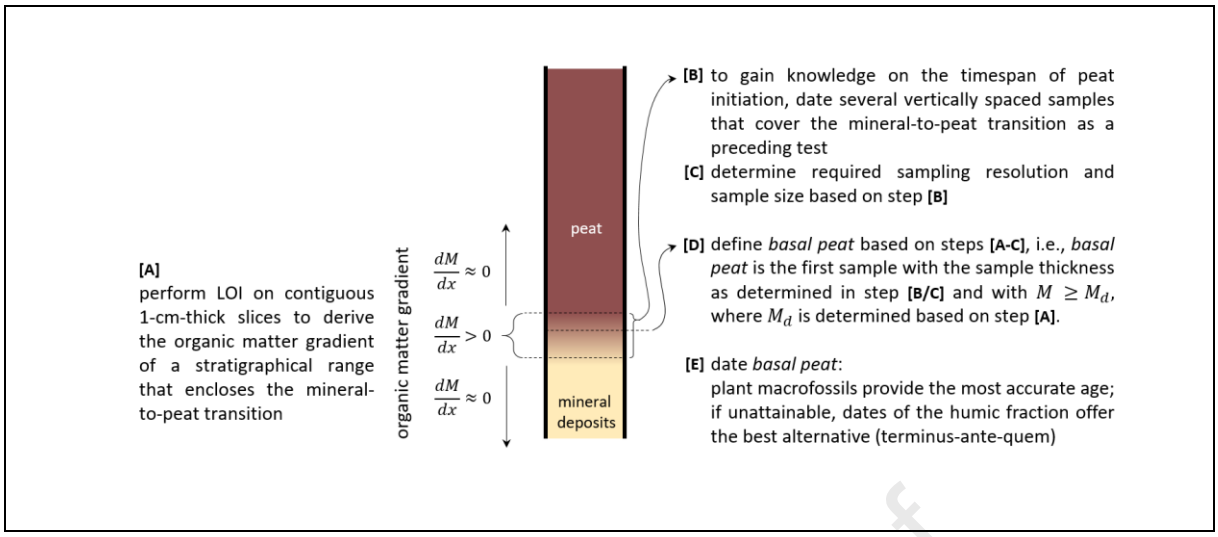

5 Conclusions

5.1 Dating peat initiation

In this study we aimed to formulate updated recommendations for dating peat initiation. We based our approach on a conceptual framework (fig. 1) that supports the use of the organic matter (OM) gradient for a quantitative and reproducible definition of the mineral-to-peat transition (i.e., the stratigraphical range reflecting the timespan of the peat initiation process) and the layer defined as *basal peat* (i.e., the stratigraphical layer that is defined as the bottom of a peat deposit). Subsequently we analysed the mineral-to-peat transition for a case study peatland in the Netherlands, based on three detailed series of radiocarbon dates that include plant macrofossils, humics and humins. Our findings demonstrate that plant macrofossils, even though their presence in basal peat is often limited, provide the most reliable dating results. If insufficient plant macrofossils are retrieved, the humic fraction provides the best alternative for dating, however dating results are most safely interpreted as a terminus-ante-quem for peat initiation. The potential large age difference between dates of plant macrofossils and humic or humin dates (up to ~1700 years between macrofossil and humic ages, and with even larger differences for humins) indicates that studies reusing existing bulk dates of *basal peat* should take great care in data interpretation. The potentially long timespan of the peat initiation process (with medians of ~1000, ~1300 and ~1500 years within our case study peatland) demonstrates that choices regarding sampling size and resolution need to be well substantiated. Our findings are summarised as a set of recommendations for dating *basal peat* in textbox 1.

5.2 Palaeoenvironment

Our case study peatland in the Netherlands currently harbours a bog vegetation, but biostratigraphical analyses show that during peat initiation the vegetation was mesotrophic. This vegetation was dominated by sedges, with some presence of *Juncus*. The data indicate that the peat initiation process initially involved fluctuating water tables and that wetter and drier conditions probably alternated. Frequent presence of charred plant remains demonstrates that wildfires occurred regularly. After the peat initiation process, conditions became more

oligotrophic, and the vegetation developed probably to an oligotrophic bog with *Calluna vulgaris*, *Erica tetralix* and *Sphagnum* at two of the studied locations and to a moss (*Bryales*) and heather vegetation at the third location.

6 Data availability:

All data from this study are available under CC-BY-SA 4.0 license at the 4TU.Centre for Research Data; see Quik *et al.* (****).

7 Author contributions

RvB secured funding for this research. CQ proposed the research outline, which was further improved based on feedback by JW, JC, BM, YvdV, and RvB. JC and CQ explored the study area, performed test corings and decided upon a coring strategy. CQ organised the fieldwork and completed the collection of data and cores in the field with help of several students (see acknowledgements). CQ coordinated all subsequent analyses that were performed on the obtained cores. Cores were opened and subsampled by MvdL and CQ. LK performed the microscopy work for analyses of plant macro remains and selection of datable material. MvdL interpreted and reported the resulting vegetation data. GS analysed the subsamples for testate amoebae. CQ performed the majority of LOI analyses, a small part of the subsamples were analysed by the CBLB (see acknowledgements). SP worked on the radiocarbon dating at the CIO laboratory in Groningen. All resulting data were combined and analysed by CQ. CQ wrote the main body of text, with input from the reports by MvdL and GS, and from discussions with JW, JC, BM, YvdV and RvB. The manuscript was finalized based on feedback from all authors.

8 Competing interests

The authors declare that they have no conflict of interest.

9 Acknowledgements

This research is part of the research programme *Home Turf - An integrated approach to Dutch raised* bogs, funded by the Netherlands Organization for Scientific Research (NWO) under grant number: 276-60-003. We thank Roos Veeneklaas (Natuurmonumenten Noordenveld) for permission to do fieldwork at the Fochteloërveen and for sharing detailed field knowledge; Hans Beens (Staatsbosbeheer Kop van Drenthe) for providing access to private roads to be able to reach the field sites; Teun Fiers, Klais Blaauw, Tom Harkema, Marte Stoorvogel, and Gibran Leeflang for field assistance; Mieke Hannink for administrative assistance with organising the fieldwork; Marcello Novani (Laboratory for Geo-information Science, WUR) for providing GNSS equipment; Jim Quik for construction work for core transport; Wouter van der Meer (BIAX Consult) for his help with opening and subsampling the cores; Harm Goorens for assistance with LOI analyses at the Soil Hydro Physics Lab (WUR) and Piet Peters for providing storage space in the cool room; Anne Roepert and colleagues of the CBLB for LOI analyses; Romy Koudijs for sharing OM data on the five duplicate cores; and Bas van Geel for his kind introduction to analysis of plant macrofossils. We thank Julie Loisel and an anonymous reviewer for their constructive comments to an earlier version of this manuscript; their feedback was much appreciated.

883
884
885 **10 References**

886 Aaby B. 1986. Palaeoecological studies of mires. In *Handbook of Holocene Palaeoecology and Palaeohydrology*,
887 Berglund BE (ed.).J. Wiley: Chichester; New York; 145–164.
888 AHN. 2021a. De details van het Actueel Hoogtebestand Nederland [Details of the Digital Elevation Model of The
889 Netherlands]. Available at:
890 https://ahn.maps.arcgis.com/apps/Cascade/index.html?appid=75245be5e0384d47856d2b912fc1b7ed
891 AHN. 2021b. Kwaliteitsbeschrijving Actueel Hoogtebestand Nederland [Quality description Digital Elevation
892 Model of The Netherlands] Available at: https://www.ahn.nl/kwaliteitsbeschrijving [Accessed 11 October
893 2021]
894 Almquist-Jacobson H, Foster DR. 1995. Toward an integrated model for raised-bog development: Theory and
895 field evidence. *Ecology* **76** (8): 2503–2516 DOI: 10.2307/2265824
896 Anderberg A-L. 1994. *Atlas of Seeds and Small Fruits of Northwest-European Plant Species; Part 4: Resedaceae-*
897 *Umbelliferae*. Edited by the Swedish Natural Science Research Council. Statens naturvetenskapliga
898 forskningaråd: Stockholm.
899 Bayliss A. 2009. Rolling out revolution: using radiocarbon dating in archaeology. *Radiocarbon* **51** (1): 123–147
900 Bayliss A, McCormac G, Van der Plicht H. 2004. An illustrated guide to measuring radiocarbon from
901 archaeological samples. *Physics Education* **39** (2): 1–8 DOI: 10.1088/0031-9120/39/2/001
902 Berendsen HJA, Makaske B, Van de Plassche O, Van Ree MHM, Das S, Van Dongen M, Ploumen S,
903 Schoenmakers W. 2007. New groundwater-level rise data from the Rhine-Meuse delta - Implications for
904 the reconstruction of Holocene relative mean sea-level rise and differential land-level movements.
905 *Geologie en Mijnbouw/Netherlands Journal of Geosciences* **86** (4): 333–354 DOI:
906 10.1017/s0016774600023568
907 Berggren G. 1969. *Atlas of Seeds and Small Fruits of Northwest-European Plant Species; Part 2: Cyperaceae*.
908 Edited by the Swedish Natural Science Research Council. Statens naturvetenskapliga forskningaråd:
909 Stockholm.
910 Berggren G. 1981. *Atlas of Seeds and Small Fruits of Northwest-European Plant Species; Part 3: Salicaceae-*
911 *Cruciferae*. Edited by the Swedish Natural Science Research Council. Statens naturvetenskapliga
912 forskningaråd: Stockholm.
913 Blaauw M, van der Plicht J, van Geel B. 2004. Radiocarbon dating of bulk peat samples from raised bogs: Non-
914 existence of a previously reported 'reservoir effect'? *Quaternary Science Reviews* **23**: 1537–1542 DOI:
915 10.1016/j.quascirev.2004.04.002
916 Booth RK, Lamentowicz M, Charman DJ. 2010. Preparation and analysis of testate amoebae in peatland
917 palaeoenvironmental studies. *Mires and Peat* **7** (2): 1–7
918 Bos IJ. 2010. Architecture and facies distribution of organic-clastic lake fills in the fluvio-deltaic Rhine-Meuse
919 system, The Netherlands. *Journal of Sedimentary Research* **80**: 339–356 DOI: 10.2110/jsr.2010.035
920 Bos IJ, Busschers FS, Hoek WZ. 2012. Organic-facies determination: A key for understanding facies distribution

in the basal peat layer of the Holocene Rhine-Meuse delta, The Netherlands. *Sedimentology* **59** (2): 676–703 DOI: 10.1111/j.1365-3091.2011.01271.x

Bosch JHA. 1990. *Assen West (12W), Assen Oost (12O). Toelichtingen bij de geologische kaart van Nederland 1:50.000.* Rijks Geologische Dienst: Haarlem.

Breuning-Madsen H, Bird KL, Balstrøm T, Elberling B, Kroon A, Lei EB. 2018. Development of plateau dunes controlled by iron pan formation and changes in land use and climate. *Catena* **171**: 580–587 DOI: 10.1016/j.catena.2018.07.011

Brock F, Lee S, Housley RA, Bronk Ramsey C. 2011. Variation in the radiocarbon age of different fractions of peat: A case study from Ahrenshöft, northern Germany. *Quaternary Geochronology* **6** (6): 550–555 DOI: 10.1016/j.quageo.2011.08.003

Bronk Ramsey C. 1995. Radiocarbon Calibration and Analysis of Stratigraphy: The OxCal Program. *Radiocarbon* **37** (2): 425–430 DOI: 10.1017/s0033822200030903

Bronk Ramsey C. 2008a. Radiocarbon dating: Revolutions in understanding. *Archaeometry* **50** (2): 249–275 DOI: 10.1111/j.1475-4754.2008.00394.x

Bronk Ramsey C. 2008b. Deposition models for chronological records. *Quaternary Science Reviews* **27**: 42–60 DOI: 10.1016/j.quascirev.2007.01.019

Bronk Ramsey C. 2009. Dealing with outliers and offsets in radiocarbon dating. *Radiocarbon* **51** (3): 1023–1045 DOI: 10.1017/s0033822200034093

Cappers RTJ, Bekker RM, Jans JEA. 2006. *Digitale zadenatlas van Nederland*. Barkhuis Publishing & Groningen University Library: Eelde, Groningen.

Chambers FM, Beilman DW, Yu Z. 2011. - Methods for determining peat humification and for quantifying peat bulk density. *Mires and Peat* **7** (7): 1–10 Available at: http://www.mires-and-peat.net/pages/volumes/map07/map0707.php

Chapman H, Gearey BR, Bamforth M, Bermingham N, Marshall P, Powlesland I, Taylor M, Whitehoude N. 2013. *Modelling archaeology and palaeoenvironments in wetlands: the hidden landscape archaeology of Hatfield and Thorne Moors, eastern England*. Available at: https://www.oxbowbooks.com/oxbow/modelling-archaeology-and-palaeoenvironments-in-wetlands.html

Charman D. 2002a. Peat and peatlands. In *Peatlands and Environmental Change*, Charman D (ed.).John Wiley & Sons, Ltd: Chichester; 3–23.

Charman D. 2002b. Origins and Peat Initiation. In *Peatlands and Environmental Change*, Charman D (ed.).John Wiley & Sons, Ltd: Chichester; 73–91.

Charman D. 2002c. Autogenic Change. In *Peatlands and Environmental Change*, Charman D (ed.).John Wiley & Sons, Ltd: Chichester; 143–165.

Cook GT, Dugmore AJ, Shore JS. 1998. The influence of pretreatment on humic acid yield and 14C age of carex peat. *Radiocarbon* **40** (1): 21–27 DOI: 10.1017/s0033822200017835

Cubizolle H, Bonnel P, Oberlin C, Tourman A, Porteret J. 2007. Advantages and limits of radiocarbon dating applied to peat inception during the end of the Late Glacial and the Holocene: The example of mires in

959 the eastern Massif Central (France). *Quaternaire* **18** (2): 187–208 DOI: 10.4000/quaternaire.1049
960 De Bakker H, Schelling J. 1966. *Systeem van bodemclassificatie voor Nederland: De hogere niveaus.* Stichting
961 voor Bodemkartering, Pudoc: Wageningen.
962 De Vleeschouwer F, Chambers FM, Swindles GT. 2010. Coring and sub-sampling of peatlands for
963 palaeoenvironmental research. *Mires and Peat* **7**: 1–10
964 Dee MW, Palstra SWL, Aerts-Bijma AT, Bleeker MO, De Bruijn S, Ghebru F, Jansen HG, Kuitems M, Paul D, Richie
965 RR, et al. 2020. Radiocarbon dating at Groningen: New and updated chemical pretreatment procedures.
966 *Radiocarbon* **62** (1): 63–74 DOI: 10.1017/RDC.2019.101
967 Douwes R, Straathof N. 2019. 14. Het Fochteloërveen. In *Hoogvenen: Landschapsecologie, Behoud, Beheer,*
968 *Herstel*, Jansen A, , Grootjans A (eds).Noordboek Natuur: Gorredijk; 133–147.
969 Edvardsson J, Poska A, Van der Putten N, Rundgren M, Linderson H, Hammarlund D. 2014. Late-Holocene
970 expansion of a south Swedish peatland and its impact on marginal ecosystems: Evidence from
971 dendrochronology, peat stratigraphy and palaeobotanical data. *Holocene* **24** (4): 466–476 DOI:
972 10.1177/0959683613520255
973 Eijkelkamp Agrisearch Equipment. 2022. Percussion drilling equipment: 1–4 Available at:
974 https://en.eijkelkamp.com/products/augering-soil-sampling-equipment/percussion-drilling-set-gasoline-
975 percussion-hammer.html [Accessed 16 February 2022]
976 Eijkelkamp Soil & Water. 2018. Peat sampler. Eijkelkamp Soil & Water, Giesbeek. Available at:
977 http://www.vanwalt.com/sediment-sampling-gouges-augers.html#PeatSamplerSet
978 Gerding M. 1995. Vier eeuwen turfwinning, De ververeningen in Groningen, Friesland, Drenthe en Overijssel
979 tussen 1550 en 1950.Wageningen University, Wageningen.
980 Givelet N, Le Roux G, Cheburkin A, Chen B, Frank J, Goodsite ME, Kempter H, Krachler M, Noernberg T, Rausch
981 N, et al. 2004. Suggested protocol for collecting, handling and preparing peat cores and peat samples for
982 physical, chemical, mineralogical and isotopic analyses. *Journal of Environmental Monitoring* **6**: 481–492
983 DOI: 10.1039/b401601g
984 Goh KM, Molloy BPJ. 1978. Radiocarbon dating of paleosols using soil organic matter components. *Journal of*
985 *Soil Science* **29**: 567–573 DOI: 10.1111/j.1365-2389.1978.tb00805.x
986 Gorham E, Lehman C, Dyke A, Janssens J, Dyke L. 2007. Temporal and spatial aspects of peatland initiation
987 following deglaciation in North America. *Quaternary Science Reviews* **26** (3–4): 300–311 DOI:
988 10.1016/j.quascirev.2006.08.008
989 Hammond AP, Goh KM, Tonkin PJ, Manning MR. 1991. Chemical pretreatments for improving the radiocarbon
990 dates of peats and organic silts in a gley podzol environment: Grahams Terrace, North Westland. *New*
991 *Zealand Journal of Geology and Geophysics* **34**: 191–194 DOI: 10.1080/00288306.1991.9514456
992 Holmquist JR, Finkelstein SA, Garneau M, Massa C, Yu Z, MacDonald GM. 2016. A comparison of radiocarbon
993 ages derived from bulk peat and selected plant macrofossils in basal peat cores from circum-arctic
994 peatlands. *Quaternary Geochronology* **31**: 53–61 DOI: 10.1016/j.quageo.2015.10.003
995 Hughes PDM. 2000. A reappraisal of the mechanisms leading to ombrotrophy in British raised mires. *Ecology*
996 *Letters* **3**: 7–9 DOI: 10.1046/j.1461-0248.2000.00118.x

997 Hughes PDM, Barber KE. 2004. Contrasting pathways to ombrotrophy in three raised bogs from Ireland and
998 Cumbria, England. *Holocene* **14** (1): 65–77 DOI: 10.1191/0959683604hl690rp
999 Iversen CM, Sloan VL, Sullivan PF, Euskirchen ES, Mcguire AD, Norby RJ, Walker AP, Warren JM, Wullschleger
1000 SD. 2015. The unseen iceberg: Plant roots in arctic tundra. *New Phytologist* **205**: 34–58 DOI:
1001 10.1111/nph.13003
1002 Joosten H, Clarke D. 2002. *Wise use of mires and peatlands - Background and principles including a framework*
1003 *for decision-making*. International Mire Conservation Group (IMCG) & International Peatland Society
1004 (IPS).
1005 Jull A, Burr G. 2015. Accelerator Mass Spectrometry. In *Encyclopedia of Scientific Dating Methods*3–6. DOI:
1006 10.1007/978-94-007-6304-3
1007 Kennedy DM, Woods JLD. 2013. *Determining Organic and Carbonate Content in Sediments*. Elsevier Ltd. DOI:
1008 10.1016/B978-0-12-374739-6.00389-4
1009 Kilian M, van der Plicht J, van Geel B. 1995. Dating raised bogs: new aspects of AMS 14C wiggle matching, a
1010 reservoir effect and climatic change. *Quaternary Science Reviews* **14**: 959–966
1011 KNMI. 2021. Klimaattabel Station Eelde, periode 1991-2020: 1
1012 Kohzu A, Matsui K, Yamada T, Sugimoto A, Fujita N. 2003. Significance of rooting depth in mire plants: Evidence
1013 from natural 15N abundance. *Ecological Research* **18**: 257–266 DOI: 10.1046/j.1440-1703.2003.00552.x
1014 Körber-Grohne U. 1964. *Bestimmungsschlüssel für subfossile Juncus-Samen und Gramineen-Früchte*.
1015 Hildesheim.
1016 Körber-Grohne U. 1991. Bestimmungsschlüssel für subfossile Gramineen-Früchte. *Probleme der*
1017 *Küstenforschung im südlichen Nordseegebiet* **18**
1018 Korhola A. 1994. Radiocarbon evidence for rates of lateral expansion in raised mires in southern Finland.
1019 *Quaternary Research* **42**: 299–307
1020 Koster E. 2005. Aeolian Environments. In *Physical Geography of Western Europe*, Koster EA (ed.).Oxford
1021 University Press: Oxford; 139–160.
1022 Koster EA. 1988. Ancient and modern cold-climate aeolian sand deposition: a review. *Journal of Quaternary*
1023 *Science* **3**: 69–83
1024 Loisel J, Bunsen M. 2020. Abrupt fen-bog transition across southern Patagonia: Timing, causes, and impacts on
1025 carbon sequestration. *Frontiers in Ecology and Evolution* **8**: 1–19 DOI: 10.3389/fevo.2020.00273
1026 Loisel J, Yu Z, Parsekian A, Nolan J, Slater L. 2013. Quantifying landscape morphology influence on peatland
1027 lateral expansion using ground-penetrating radar (GPR) and peat core analysis. *Journal of Geophysical*
1028 *Research: Biogeosciences* **118**: 373–384 DOI: 10.1002/jgrg.20029
1029 Macdonald GM, Beilman DW, Kremenetski KV, Sheng Y, Smith LC, Velichko AA. 2006. Rapid early development
1030 of circumarctic peatlands and atmospheric CH4 and CO2 variations. *Science* **314**: 285–288 DOI:
1031 10.1126/science.1131722
1032 Mäkilä M. 1997. Holocene lateral expansion, peat growth and carbon accumulation on Haukkasuo, a raised bog
1033 in southeastern Finland. *Boreas* **26** (1): 1–14 DOI: 10.1111/j.1502-3885.1997.tb00647.x
1034 Ministerie van Economische Zaken. 2018. Natura 2000-gebieden peildatum 27 augustus 2018 [Data File]

Ministerie van Verkeer en Waterstaat. 2007. Landelijke CONCEPT dataset lijnvormige waterlichamen status mrt 2007 [Data file]

Moore P. 1993. The origin of blanket mire, revisited. In *Climate Change and Human Impact on the Landscape*, Chambers F (ed.).Chapman and Hal: London; 217–224.

Moore PD. 1975. Origin of blanket mires. *Nature* **256** (5515): 267–269 DOI: 10.1038/256267a0

Morris PJ, Swindles GT, Valdes PJ, Ivanovic RF, Gregoire LJ, Smith MW, Tarasov L, Haywood AM, Bacon KL. 2018. Global peatland initiation driven by regionally asynchronous warming. *Proceedings of the National Academy of Sciences of the United States of America* **115** (19): 4851–4856 DOI: 10.1073/pnas.1717838115

Nelson K, Thompson D, Hopkinson C, Petrone R, Chasmer L. 2021. Peatland-fire interactions: A review of wildland fire feedbacks and interactions in Canadian boreal peatlands. *Science of the Total Environment* **769**: 1–14 DOI: 10.1016/j.scitotenv.2021.145212

Nilsson M, Klarqvist M, Bohlin E, Possnert G. 2001. Variation in 14C age of macrofossils and different fractions of minute peat samples dated by AMS. *Holocene* **11** (5): 579–586 DOI: 10.1191/095968301680223521

Palstra SWL, Wallinga J, Viveen W, Schoorl JM, Van den Berg M, Van der Plicht J. 2021. Cross-comparison of last glacial radiocarbon and OSL ages using periglacial fan deposits. *Quaternary Geochronology* **61** DOI: 10.1016/j.quageo.2020.101128

Philippsen B. 2013. The freshwater reservoir effect in radiocarbon dating. *Heritage Science* **1** (24): 1–19 DOI: 10.1186/2050-7445-1-24

Piotrowska N, Blaauw M, Mauquoy D, Chambers F. 2011. Constructing deposition chronologies for peat deposits using radiocarbon dating. *Mires and Peat* **7**: 1–14 Available at: http://www.mires-and-peat.net/map07/map_07_10.pdf

Provincie Drenthe. 2016. Beheerplan Fochteloërveen - Op weg naar een levend hoogveen. Provincie Drenthe, Assen.

Quik C, Palstra SWL, Van Beek R, Van der Velde Y, Candel JHJ, Van der Linden M, Kubiak-Martens L, Swindles G, Makaske B, Koudijs R, et al. 2022. Data from: Dating basal peat: the geochronology of peat initiation revisited DOI: 10.4121/16923358

Quik C, Velde Y van der, Harkema T, Van der Plicht H, Quik J, Beek R van, Wallinga J. 2021. Using legacy data to reconstruct the past? Rescue, rigor and reuse in peatland geochronology. *Earth Surface Processes and Landforms* **46**: 2607–2631 DOI: 10.1002/esp.5196

Rappol M. 1987. Saalian till in the Netherlands: a review. In *INQUA Symposium on the Genesis and Lithology of Glacial Deposits – Amsterdam, 1986*, Van der Meer JJM (ed.).Balkema: Rotterdam, Boston; 3–21.

Rappol M, Haldorsen S, Jørgensen P, Van der Meer JJM, Stoltenberg HMP. 1989. Composition and origin of petrographically stratified thick till in the Northern Netherlands and a Saalian glaciation model for the North Sea basin. *Mededelingen van de Werkgroep voor Tertiair en Kwartair Geologie* **26**: 31–64

Reimer P, Austin W, Bard E, Bayliss A, Blackwell P, Bronk Ramsey C, Butzin M, Cheng H, Edwards R, Friedrich M, et al. 2020. The IntCal20 Northern Hemisphere radiocarbon age calibration curve (0–55 cal kBP). *Radiocarbon* **62** (4): 725–757 DOI: 10.1017/RDC.2020.41

1073 Rein G, Huang X. 2021. Smouldering Wildfires in Peatlands, Forests and the Arctic: Challenges and Perspectives.
1074 *Current Opinion in Environmental Science & Health* DOI: 10.1016/j.coesh.2021.100296
1075 Roe HM, Charman DJ, Roland Gehrels W. 2002. Fossil testate amoebae in coastal deposits in the UK:
1076 Implications for studies of sea-level change. *Journal of Quaternary Science* **17** (5–6): 411–429 DOI:
1077 10.1002/jqs.704
1078 Ruppel M, Väliranta M, Virtanen T, Korhola A. 2013. Postglacial spatiotemporal peatland initiation and lateral
1079 expansion dynamics in North America and northern Europe. *Holocene* **23** (11): 1596–1606 DOI:
1080 10.1177/0959683613499053
1081 Rydin H, Jeglum JK. 2013a. Peatland habitats. In *The Biology of Peatlands*, Rydin H, , Jeglum JK (eds).Oxford
1082 University Press: Oxford; 1–20.
1083 Rydin H, Jeglum JK. 2013b. Peatland succession and development. In *The Biology of Peatlands*, Rydin H, ,
1084 Jeglum JK (eds).Oxford University Press: Oxford; 127–147.
1085 Rydin H, Jeglum JK. 2013c. Productivity and peat accumulation. In *The Biology of Peatlands*, Rydin H, , Jeglum JK
1086 (eds).Oxford University Press: Oxford; 254–273.
1087 Shore JS, Bartley DD, Harkness DD. 1995. Problems encountered with the 14C dating of peat. *Quaternary*
1088 *Science Reviews* **14** (4): 373–383 DOI: 10.1016/0277-3791(95)00031-3
1089 Smith AJ. 2004. *The Moss Flora of Britain and Ireland*. Cambridge University Press: Cambridge.
1090 Smolders AJP, Tomassen HBM, Pijnappel HW, Lamers LPM, Roelofs JGM. 2001. Substrate-derived CO2 is
1091 important in the development of Sphagnum spp. *New Phytologist* **152** (2): 325–332 DOI: 10.1046/j.0028-
1092 646X.2001.00261.x
1093 Straathof N, Bijkerk W, Land KA. 2017. Neergang en opkomst van het Fochteloërveen : resu ltaten van 30 iaar
1094 hoogveenherstel. (July)
1095 Streif H. 1972. The results of stratigraphical and facial investigations in the coastal Holocene of
1096 Woltzeten/Ostfriesland, Germany. *Geologiska Föreningen i Stockholm Förhandlingar* **94** (2): 281–299
1097 DOI: 10.1080/11035897209454203
1098 Sullivan ME, Booth RK. 2011. The potential influence of short-term environmental variability on the
1099 composition of testate amoeba communities in Sphagnum peatlands. *Microbial Ecology* **62** (1): 80–93
1100 Swindles GT, Roe HM. 2007. Examining the dissolution characteristics of testate amoebae (Protozoa:
1101 Rhizopoda) in low pH conditions: Implications for peatland palaeoclimate studies. *Palaeogeography,*
1102 *Palaeoclimatology, Palaeoecology* **252** (3–4): 486–496 DOI: 10.1016/j.palaeo.2007.05.004
1103 Swindles GT, Roland TP, Amesbury MJ, Lamentowicz M, McKeown MM, Sim TG, Fewster RE, Mitchell EAD.
1104 2020. Quantifying the effect of testate amoeba decomposition on peat-based water-table
1105 reconstructions. *European Journal of Protistology* **74**: 125693 DOI: 10.1016/j.ejop.2020.125693
1106 Synal HA, Stocker M, Suter M. 2007. MICADAS: a new compact radiocarbon AMS system. *Nuclear Instruments*
1107 *and Methods* **B259**: 7–13
1108 Ter Wee M. 1972. Geologische opbouw van Drenthe. Rijks Geologische Dienst, Haarlem.
1109 Ter Wee M. 1979. *Emmen West (17W), Emmen Oost (17O). Toelichtingen bij de geologische kaart van*
1110 *Nederland 1:50.000*. Rijks Geologische Dienst: Haarlem.

TNO-GSN. 2021a. Basisveen Bed. *Stratigraphic Nomenclature of the Netherlands* Available at: http://www.dinoloket.nl/en/stratigraphic-nomenclature/basisveen-bed [Accessed 16 March 2021]

TNO-GSN. 2021b. Gieten Member. *Stratigraphic Nomenclature of the Netherlands* Available at: http://www.dinoloket.nl/en/stratigraphic-nomenclature/gieten-member [Accessed 1 April 2021]

TNO-GSN. 2021c. Laagpakket van Wierden. In: Stratigrafische Nomenclator van Nederland Available at: https://www.dinoloket.nl/en/stratigraphic-nomenclature/wierden-member [Accessed 16 March 2021]

Tolonen K, Turunen J. 1996. Accumulation rates of carbon in mires in Finland and implications for climate change. *Holocene* **6** (2): 171–178 DOI: 10.1177/095968369600600204

TOPCON. 2017. Hiper V Versatile Function GNSS Receiver. TOPCON Corporation.

Törnqvist TE, Hijma MP. 2012. Links between early Holocene ice-sheet decay, sea-level rise and abrupt climate change. *Nature Geoscience* **5** (9): 601–606 DOI: 10.1038/ngeo1536

Törnqvist TE, De Jong AFM, Oosterbaan WA, Van Der Borg K. 1992. Accurate dating of organic deposits by AMS 14C measurement of macrofossils. *Radiocarbon* **34** (3): 566–577 DOI: 10.1017/S0033822200063840

Törnqvist TE, Rosenheim BE, Hu P, Fernandez AB. 2015. Radiocarbon dating and calibration. In *Handbook of Sea-Level Research*, Shennan I, , Long AJ, , Horton BP (eds).John Wiley & Sons, Ltd; 349–360. DOI: 10.1002/9781118452547.ch23

Törnqvist TE, Van Ree MHM, Van 't Veer R, Van Geel B. 1998. Improving Methodology for High-Resolution Reconstruction of Sea-Level Rise and Neotectonics by Paleoecological Analysis and AMS 14C Dating of Basal Peats. *Quaternary Research* **49**: 72–85 DOI: 10.1006/qres.1997.1938

Tuniz C, Bird JR, Fink D, Herzog GF. 1998. *Accelerator Mass Spectrometry: ultrasensitive analysis for global science*. CRC Press, Boca Raton.

Väliranta M, Salojärvi N, Vuorsalo A, Juutinen S, Korhola A, Luoto M, Tuittila ES. 2017. Holocene fen–bog transitions, current status in Finland and future perspectives. *Holocene* **27** (5): 752–764 DOI: 10.1177/0959683616670471

Van Aalst JW. 2021. OpenSimpleTopo, 3200 pixels per km (scale 1:3,125 as hardcopy), current release: 2021-R02, feb. 2021, map sheets used: 3200-11HNb, 3200-11HNd, 3200-11HZb, 3200-12CNa, 3200-12CNb, 3200-12CNc, 3200-12CNd, 3200-12CZa, 3200-12CZb Available at: www.opentopo.nl [Accessed 19 May 2021]

Van Asselen S, Cohen KM, Stouthamer E. 2017. The impact of avulsion on groundwater level and peat formation in delta floodbasins during the middle-Holocene transgression in the Rhine-Meuse delta, The Netherlands. *Holocene* **27** (11): 1694–1706 DOI: 10.1177/0959683617702224

Van Beek R, Maas GJ, Van Den Berg E. 2015. Home Turf: An interdisciplinary exploration of the long-term development, use and reclamation of raised bogs in the Netherlands. *Landscape History* **36** (2): 5–34 DOI: 10.1080/01433768.2015.1108024

Van den Berg MW, Beets DJ. 1987. Saalian glacial deposits and morphology in The Netherlands. In *INQUA Symposium on the Genesis and Lithology of Glacial Deposits – Amsterdam, 1986*, Van der Meer JJM (ed.).Balkema: Rotterdam, Boston; 235–251.

Van der Meij WM, Temme AJAM, Lin HS, Gerke HH, Sommer M. 2018. On the role of hydrologic processes in

soil and landscape evolution modeling: concepts, complications and partial solutions. *Earth-Science Reviews* **185**: 1088–1106 DOI: 10.1016/j.earscirev.2018.09.001

Van der Plicht J, Streurman H, Van Mourik J. 2019. Radiocarbon dating of soil archives. In *Reading the Soil Archives - Unravelling the Geoecological Code of Palaeosols and Sediment Cores (Developments in Quaternary Science 18)*, Van Mourik J, , Van der Meer J (eds).Elsevier B.V.; 81–113.

Van Geel B. 1978. A palaeoecological study of holocene peat bog sections in Germany and The Netherlands, based on the analysis of pollen, spores and macro- and microscopic remains of fungi, algae, cormophytes and animals. *Review of Palaeobotany and Palynology* **25** (1): 1–120 DOI: 10.1016/0034-6667(78)90040-4

Van Mourik J, Wartenbergh P, Mook W, Streurman H. 1995. Radiocarbon dating of palaeosols in aeolian sands. *Mededelingen Rijks Geologische Dienst* **52**: 425–439

Van Strydonck M. 2016. Radiocarbon Dating. *Topics in Current Chemistry* **374** (13): 1–18 DOI: 10.1007/s41061-016-0011-9

Vos P, De Vries S. 2013. 2e generatie palaeogeografische kaarten van Nederland (versie 2.0) Available at: www.cultureelerfgoed.nl [Accessed 22 January 2020]

Vos P, Van der Meulen M, Weerts H, Bazelmans J. 2020. *Atlas of the Holocene Netherlands, landscape and habitation since the last ice age*. Amsterdam University Press: Amsterdam.

Waddington JM, Roulet NT. 1997. Groundwater flow and dissolved carbon movement in a boreal peatland. *Journal of Hydrology* **191** (1–4): 122–138 DOI: 10.1016/S0022-1694(96)03075-2

Waller MP, Long AJ, Schofield JE. 2006. Interpretation of radiocarbon dates from the upper surface of late-Holocene peat layers in coastal lowlands. *Holocene* **16** (1): 51–61 DOI: 10.1191/0959683606hl895ra

Wallinga J, Van der Staay J. 1999. Sampling in waterlogged sands with a simple hand-operated corer. *Ancient TL* **17**: 59–61

Weckström J, Seppä H, Korhola A. 2010. Climatic influence on peatland formation and lateral expansion in sub-arctic Fennoscandia. *Boreas* **39** (4): 761–769 DOI: 10.1111/j.1502-3885.2010.00168.x

Wohlfarth B, Skog G, Possnert G, Holmquist B. 1998. Pitfalls in the AMS radiocarbon-dating of terrestrial macrofossils. *Journal of Quaternary Science* **13** (2): 137–145 DOI: 10.1002/(SICI)1099-1417(199803/04)13:2<137::AID-JQS352>3.0.CO;2-6

WRB-IUSS. 2015. *World Reference Base for Soil Resources. World Soil Resources Reports 106*.

Wüst RAJ, Jacobsen GE, van der Gaast H, Smith AM. 2008. Comparison of radiocarbon ages from different organic fractions in tropical peat cores: Insights from Kalimantan, Indonesia. *Radiocarbon* **50** (3): 359–372 DOI: 10.1017/S0033822200053492

Yu Z, Beilman DW, Frolking S, MacDonald GM, Roulet NT, Camill P, Charman DJ. 2011. Peatlands and their role in the global carbon cycle. *Eos* **92** (12): 1–3

Zaccone C, Rein G, Orazio VD, Hadden RM, Belcher CM, Miano TM. 2014. Smouldering fire signatures in peat and their implications for palaeoenvironmental reconstructions. *Geochimica et Cosmochimica Acta* **137**: 134–146 DOI: 10.1016/j.gca.2014.04.018

- We present three detailed radiocarbon sequences of the mineral-to-peat transition
- Basal peat needs to be clearly defined based on a quantitative reproducible parameter
- Peat initiation is a process of a certain timespan rather than an event
- Plant macrofossil dates are most accurate, humic/humin dates are likely too young
- A conceptual framework and recommendations for dating peat initiation are presented

Declaration of Competing Interests

The authors declare that they have no conflict of interest.